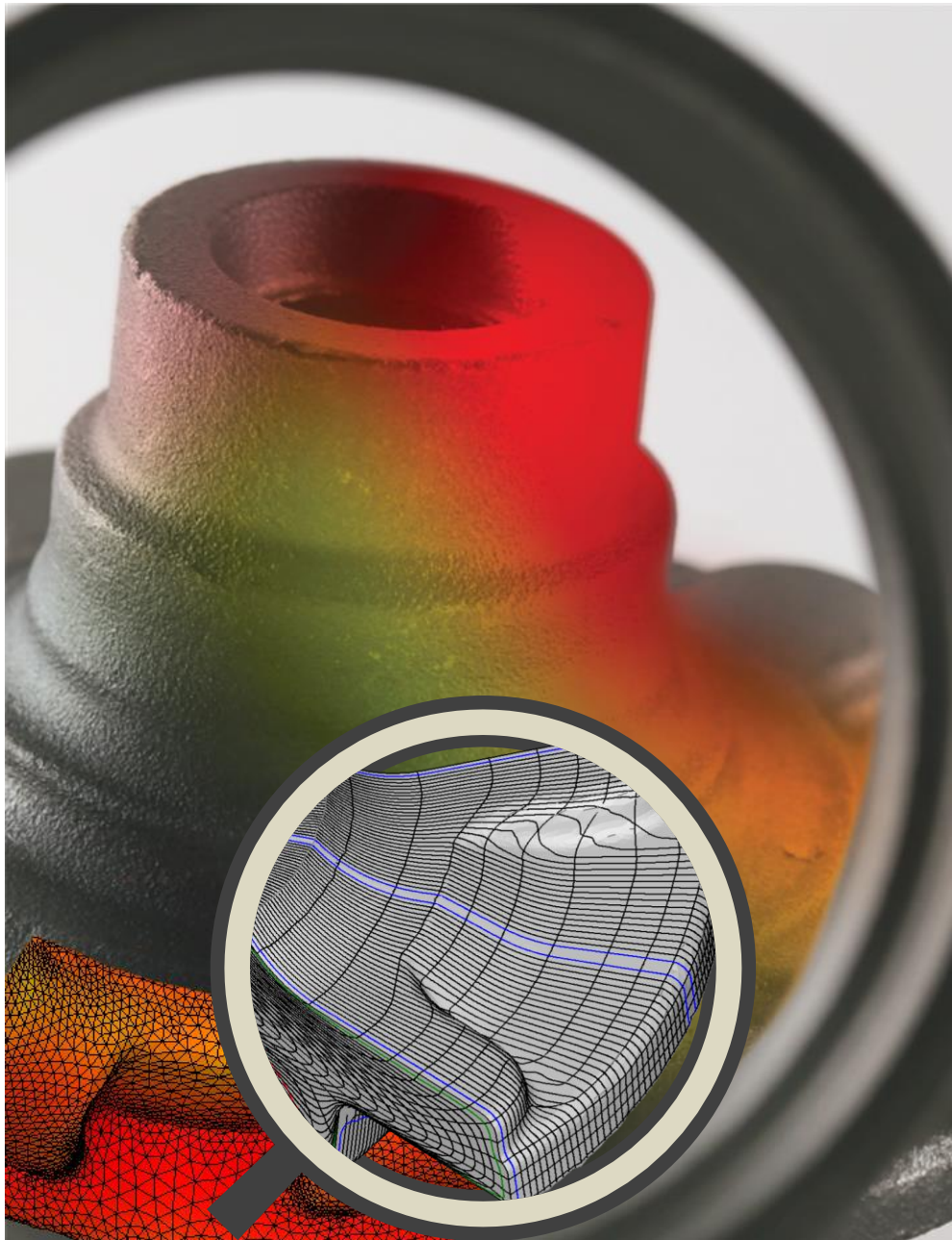
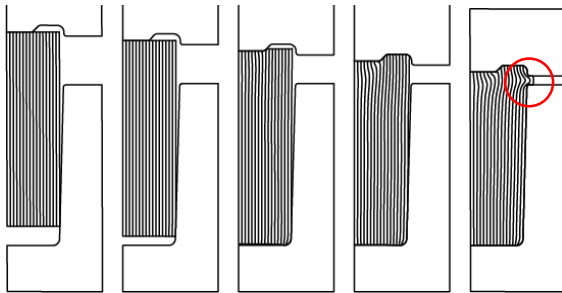


AFDEX

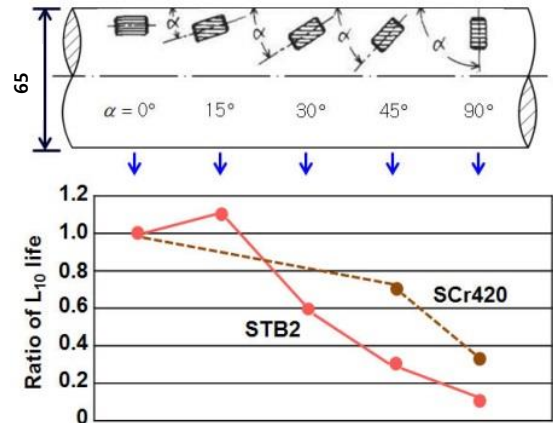
Intelligent Metal Forming Simulation Software



❖ Enhancement of Product Quality with Optimized Metal Flow Lines



Old

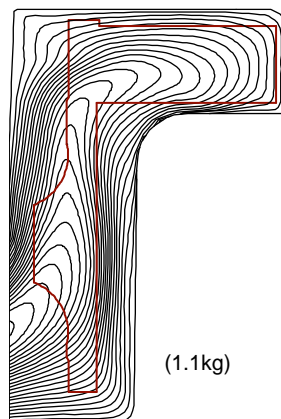


Ito, S., Tusuhima, N., Muro, H.

Metal flow lines or grain flows are very important in the lifespan of metal-formed products. Ito et al. (1982, ASTM, pp. 125-135) presented lifespan dependence of taper roller on metal flow lines (See the graph on the right). A bearing company achieved a major breakthrough in manufacturing taper rollers in the middle of 1990s using AFDEX, leading it in the years to come, to retain the world-class quality competitiveness in the taper-roller bearing industry.

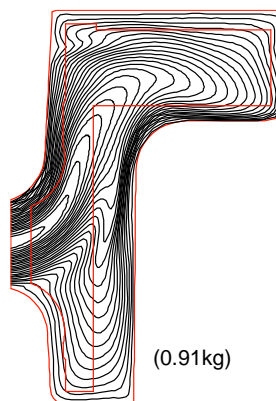
❖ Weight Minimization of Parts with Improved Product Quality

Old process design

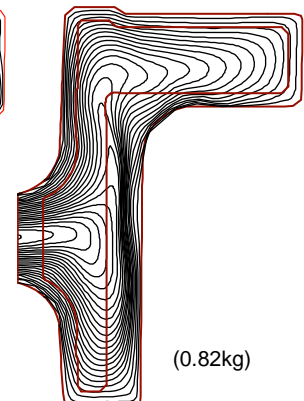


(1.1kg)

Optimized process design



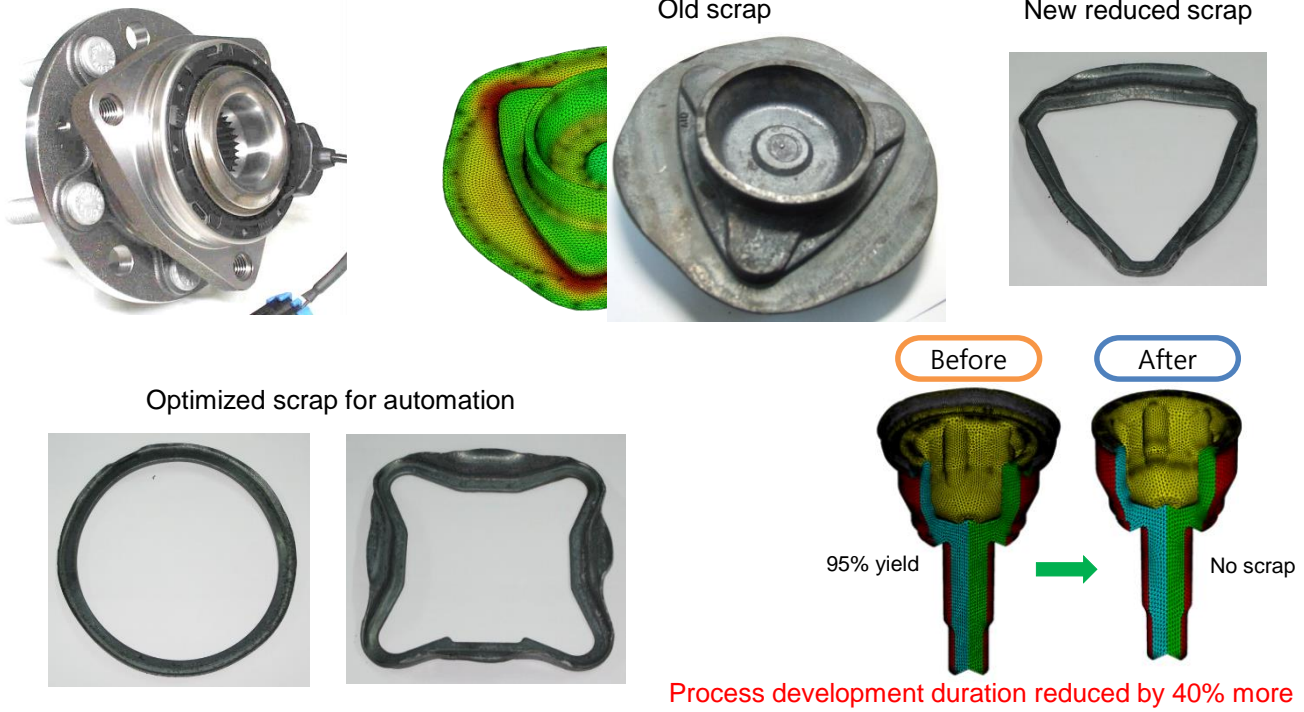
(0.91kg)



(0.82kg)

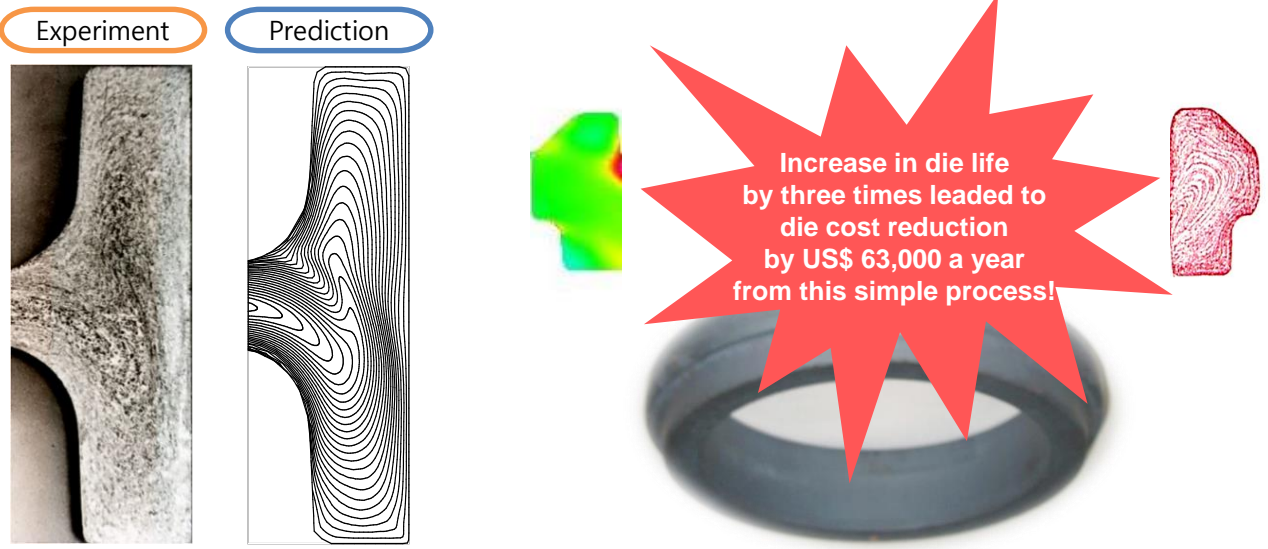
An experience-based optimization of metal-forming process is very time-demanding and costly especially when the process design engineer aims at obtaining optimized metal flow lines (see the picture on the right). This example shows a typical process design innovation through its optimization using AFDEX by a bearing manufacturer. An automobile parts vendor successfully optimized metal flow lines in the parts so as to considerably reduce its weight.

❖ Green Manufacturing and Process Optimization for Automation



AFDEX dramatically reduces the amount of useless scrap, helping users to realize process design optimization for automation, which is very complicated because of optimal process design, metal flow lines and strength. Of course, it frequently contributes to reducing total process development time by over 40%.

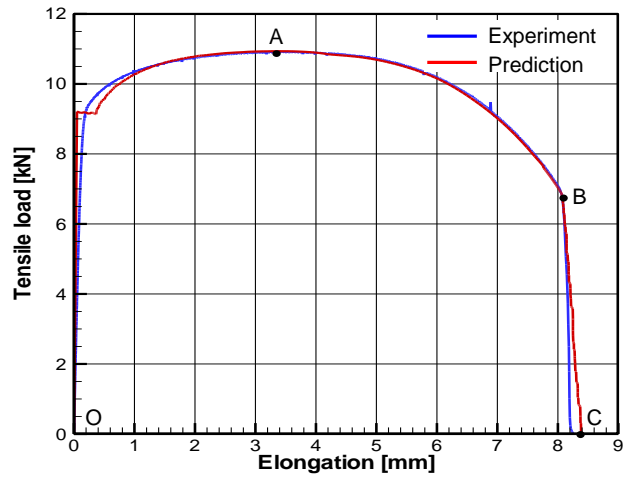
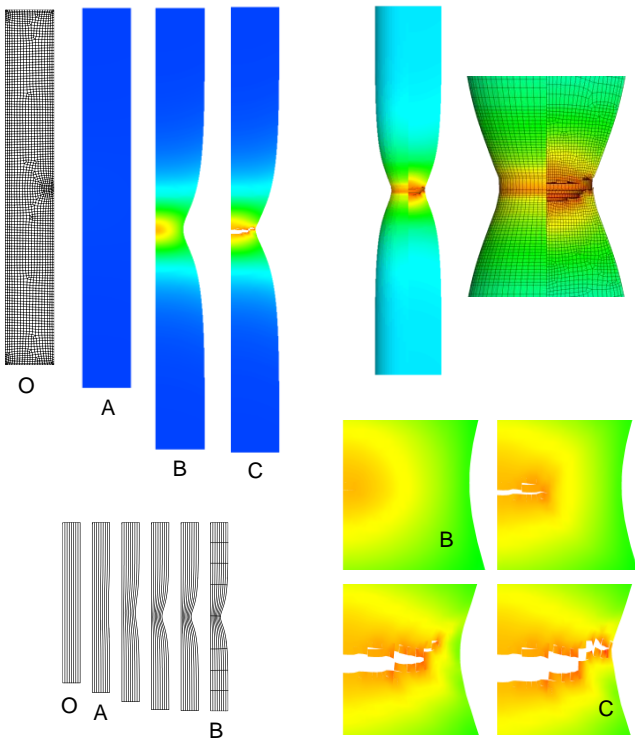
❖ Enhancement of Die Life and Reduction of Manufacturing Cost



In MFC AE 1996, one of the AFDEX users presented a success story about drastic reduction of development time from 6 months to two weeks.

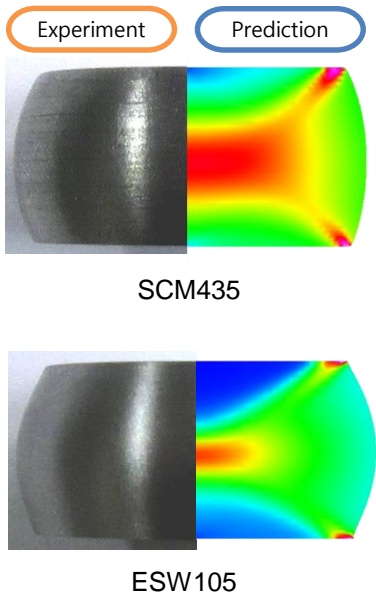
In MFC AE 2001, a user presented a success story about increased die lifespan by three times, leading to drastic reduction of die cost, i.e., US\$63,000/year in a simple and standard hot forging process of an automobile part.

❖ 2D, Tensile Testing

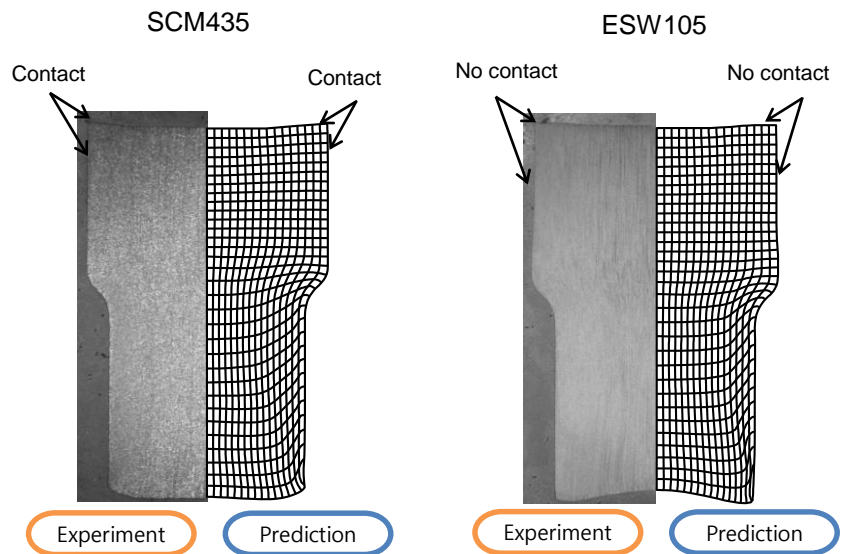


Tensile testing is one of the typical metal forming processes, which is useful for evaluating the predictions, learning principles embedded in solid mechanics and understanding material behaviors in metal forming. The graph shows the result of the entire process in a simulated tensile test including crack propagation after fracture point, revealing that the predictions are very close to that of experiments. The flow stress employed here is based on the properties given by AFDEX MAT.

❖ 2D, Upsetting, Forward Extrusion



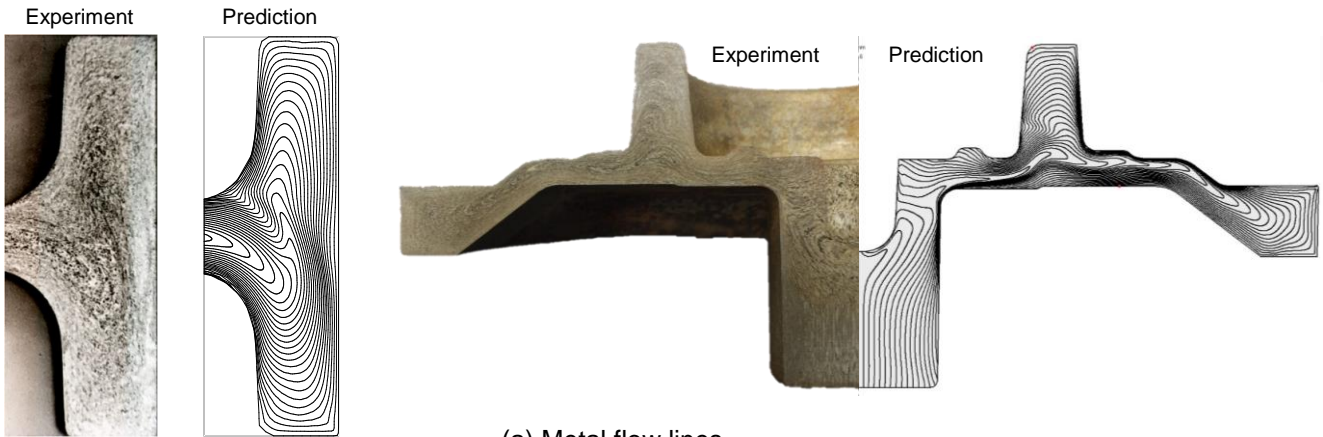
(a) Cylinder compression



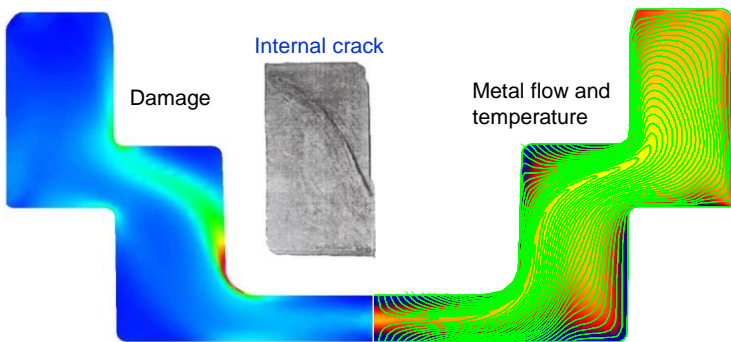
(b) Forward extrusion

Figures (a) and (b) show a comparison of deformed shapes arising in the experiments and predictions of solid cylinder compression and forward extrusion of two different materials of SCM435 and ESW105, respectively.

❖ 2D Simulation of Hot Forging, Bearing Race, Combined Gear and Shaft



(a) Metal flow lines



(b) Cracks and their possible causes

In the Figure (a), predictions compares to the experimental metal flow lines generated by automatic three-stage hot-forging and a mechanical press forging in which product quality critically depends on the soundness of the metal flow lines.

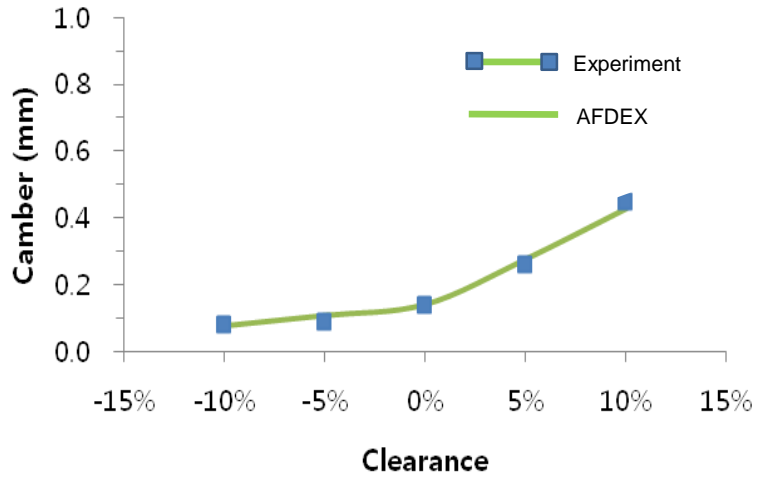
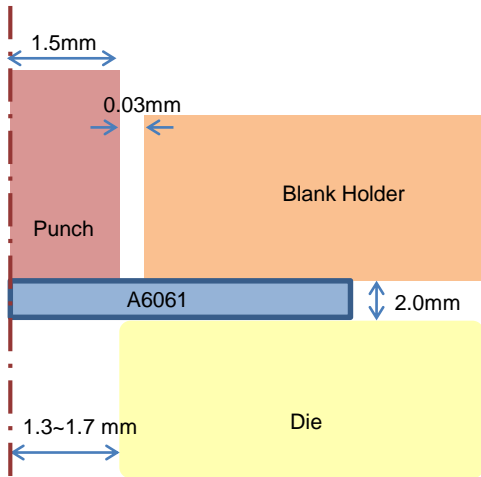
Figure (b) shows the internal cracks of the product with their possible causes easily inferred by the metal flow lines and temperature distribution.

❖ 2D, Automatic 5-stage Cold Forging, Engine Part



The figures show a comparison of the predicted results with experimental results of an automatic five-stage cold forging process. Note that the simulation of automatic multi-stage forging processes (sometimes called fastener forming processes or former processes) should be supported by more sophisticated capabilities of BMF simulators as their consecutive stages are closely related, and the die-workpiece tolerance at each stage is very tight.

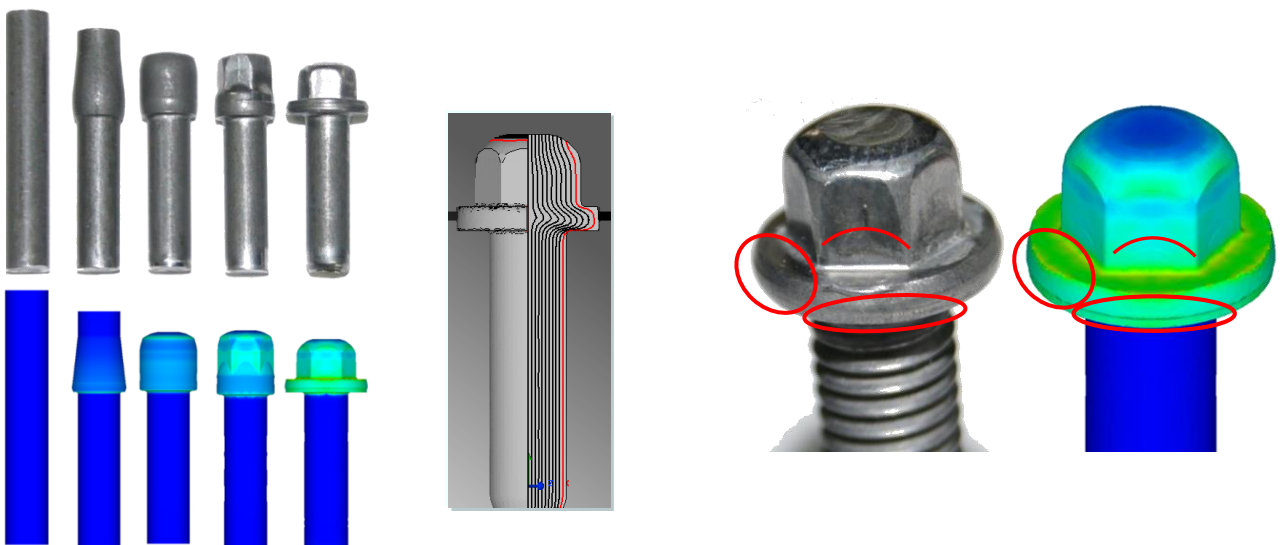
❖ 2D, Marking, Plate Forging



Parameter	Value
N	0.194
K (MPa)	207.6
Frictional coefficient	0.15
Punch speed	0.83 mm/s
Blank holder force	210.9 N

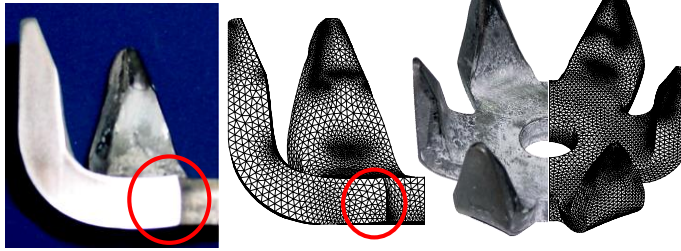
The lower right graph compares the experiments and predictions of camber in a marking process, showing that the predictions are in a good agreement with the experimental results throughout the entire range of clearance.

❖ 2D/3D Bolt Forming Simulation

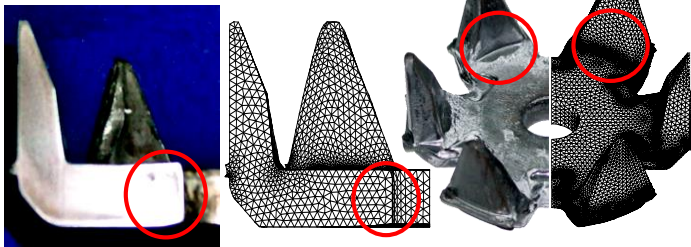


The figures show a comparison between the experiments and predictions of an automatic four-stage cold forging process for a high-strength bolt, showing that the most important features in the experiments are well reflected by the predictions.

❖ 3D, Cold Forging, Rotor Pole

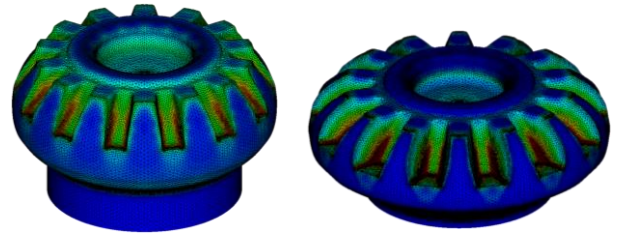


Bending process



Sizing process

❖ 3D, Enclosed-die Forging, Bevel Gear



Enclosed-die forging



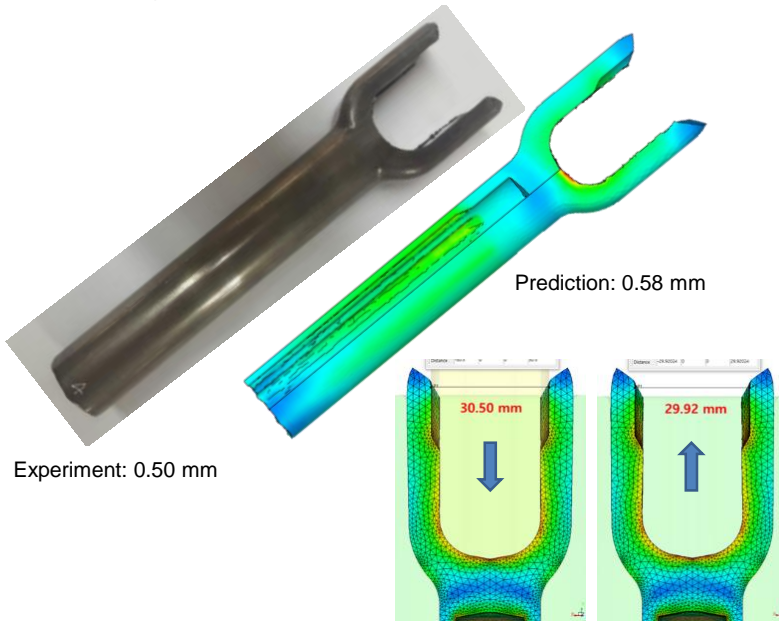
Enclosed-die forging

Sizing

Figures show a comparison of the predictions and experiments of a rotor pole, cold-forged (left), and a bevel gear, manufactured by enclosed-die forging followed by sizing (right). Note that precision simulation is required in the simulation of such a precision forging process as the enclosed die forging shown in the right figure.

❖ 3D Springback Analysis, Automatic Multi-stage Cold Forging

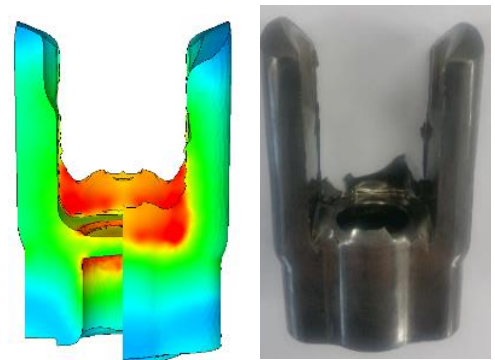
✓ Springback displacement of a yoke



Experiment: 0.50 mm

Prediction: 0.58 mm

✓ Eccentricity of a pinch yoke

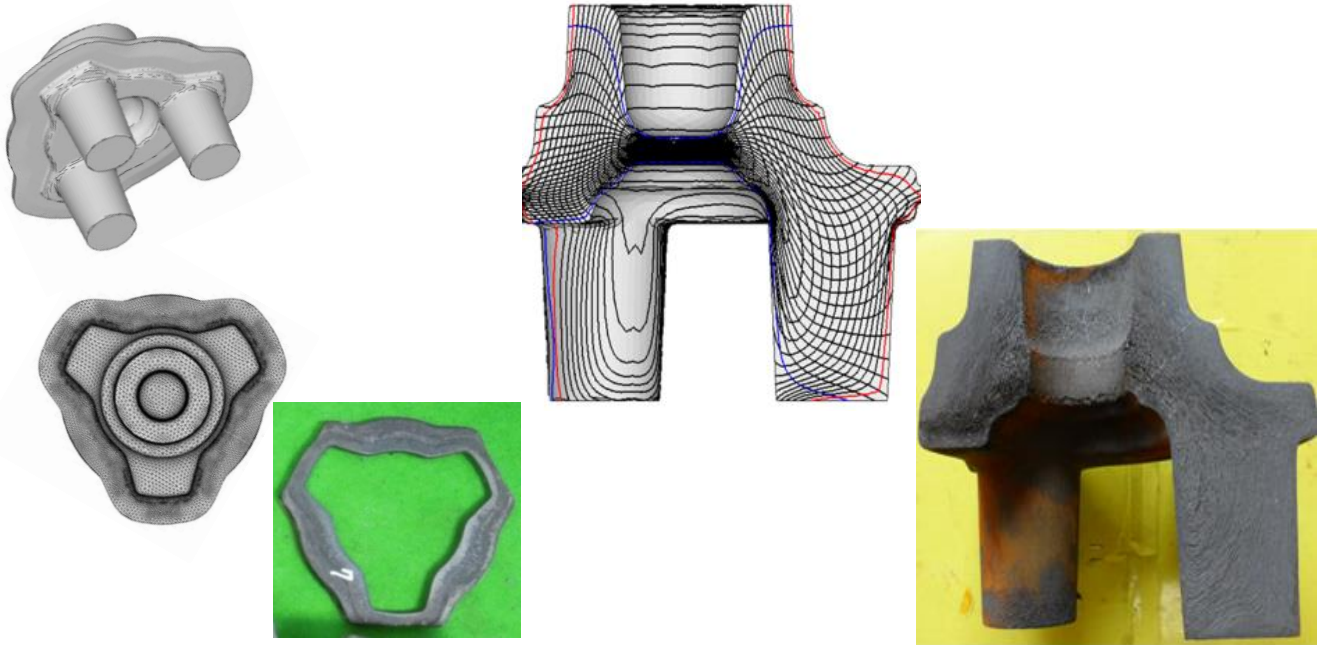


Prediction: 1.030

Experiment: 1.038

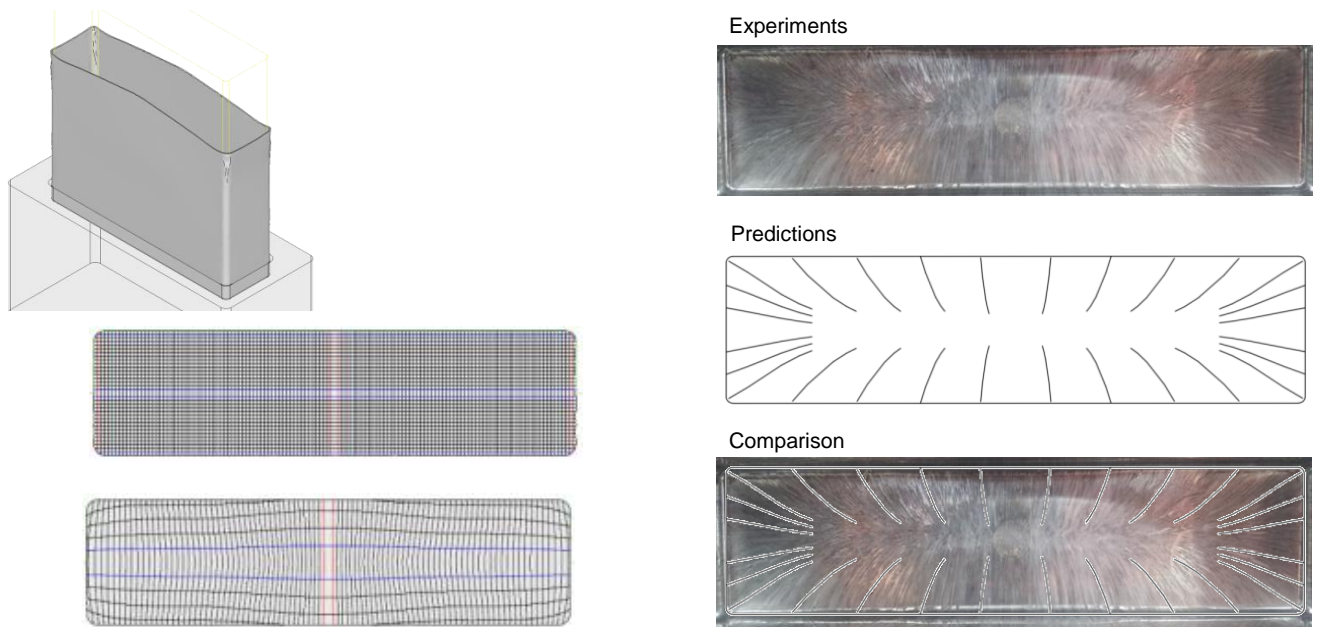
The figures show a comparison of the results of experiment and prediction of a yoke cold forging by automatic multi-stage forging machine, revealing that the predictions reflect the most important features in the experiments quite well. It is noted that ejection process was simulated to predict springback using 3D elastoplastic finite element method. The predicted springback of 0.58mm is very close to the experimental value of 0.50mm.

❖ 3D, Hot Forging, Planetary Gear Part



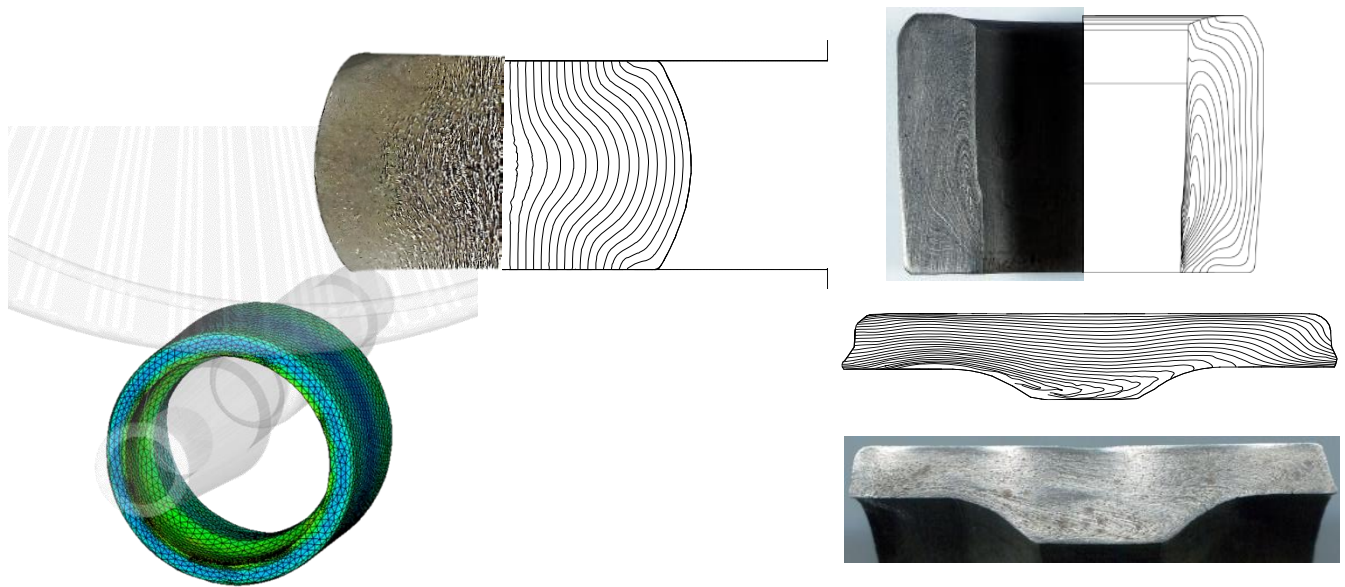
The figures show a comparison of the predictions and experiments of a planetary gear part hot forging process with emphasis on three-dimensional metal flow lines.

❖ 3D, Impact Backward Extrusion, Battery Case



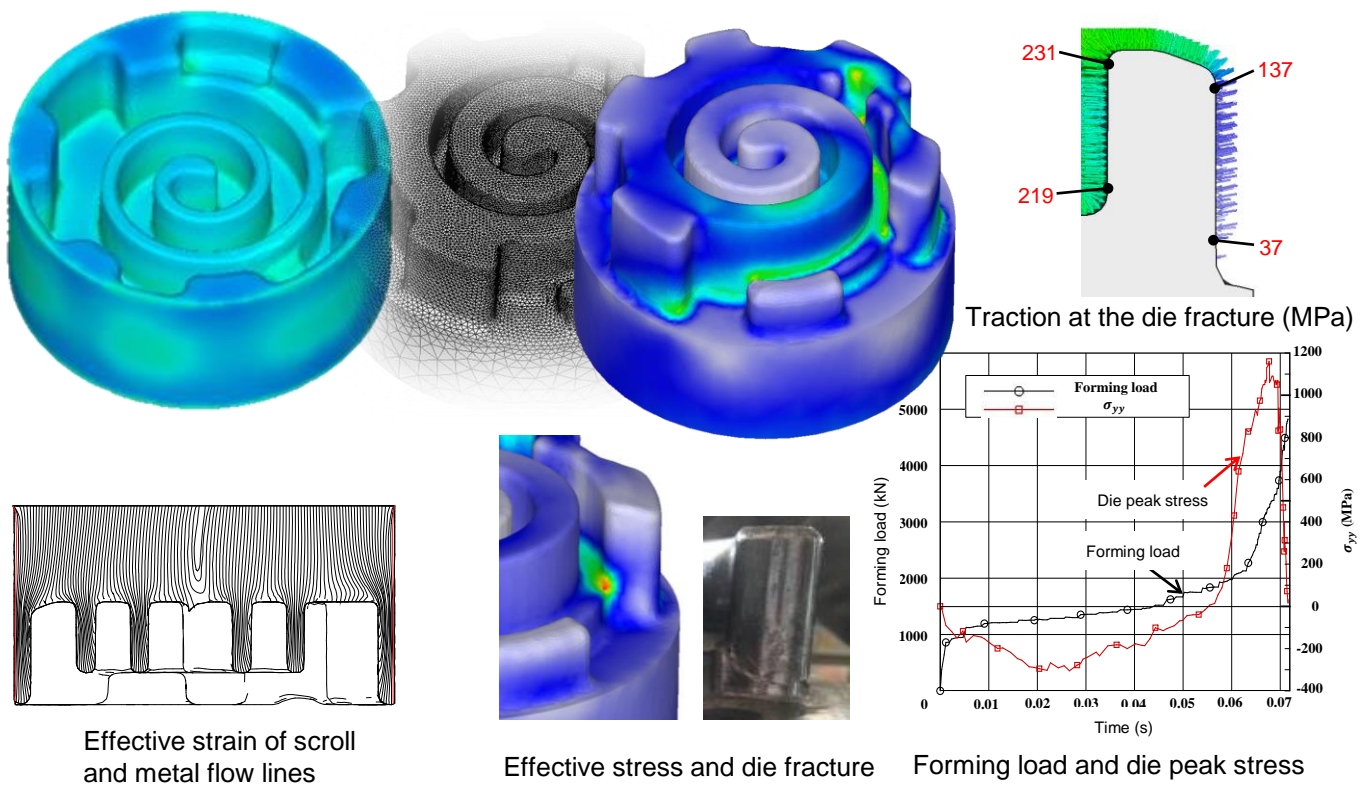
The figures show a comparison of the predictions and experiments of a battery case backward extrusion process with emphasis on path lines carved on the inner bottom. Note that this process is quite sensitive to the friction. Hybrid frictional law is recommended for this kind of process.

❖ 3D, Ring-rolling-after-forging, Bearing Race



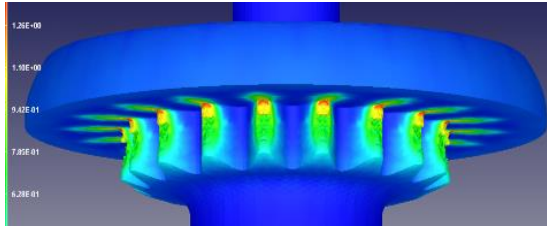
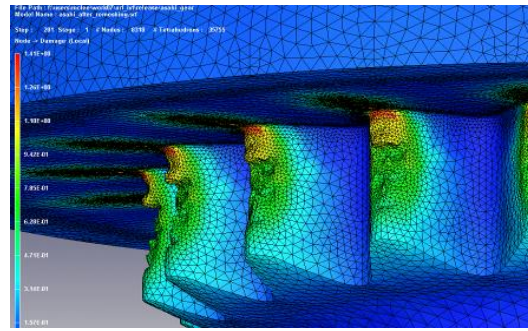
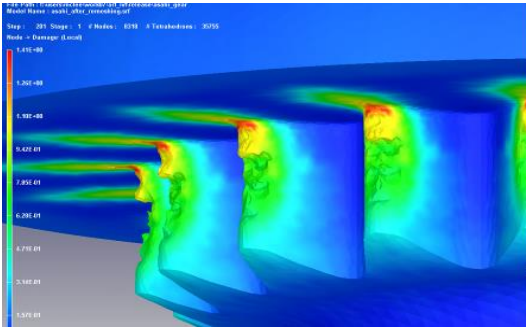
The simulation results and experiments of ring-rolling-after-hot-forging process for the first-generation hub bearing outer race are shown in the figures above, with emphasis on three-dimensional metal flow lines, revealing that the simulation results are in good agreement with the experimental results. Note that the metal flow lines are automatically traced throughout the entire process composed of upsetting, backward extrusion, piercing and ring rolling.

❖ 3D, Aluminum Hot Forging, Die Fracture Prediction, Fixed Scroll



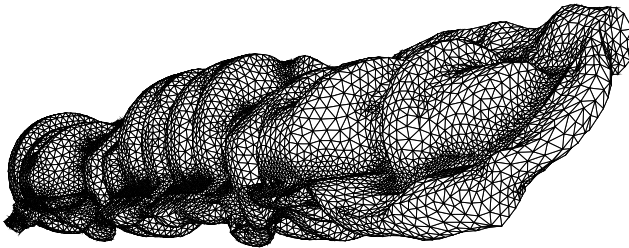
The figures show the reason of die fracture occurring in hot forging of an aluminum fixed scroll, revealing that the stress in tension near the root of the wrap before the final stroke is the direct reason of die fracture.

❖ Ductile Fracture



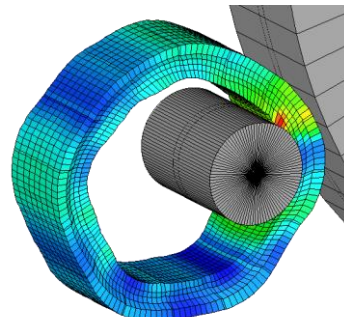
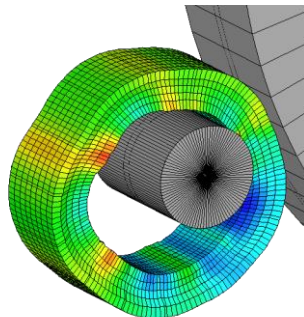
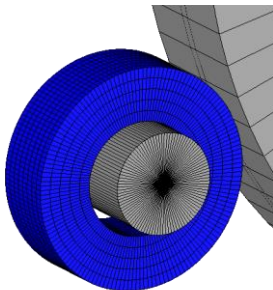
Ductile fracture is one of the complicated problems occurring in metal forming. Metal forming simulation technology leads process design engineers steadily to the phenomena and help them to accumulate the valuable knowledge and know-how in a systematic way.

❖ 3D, Hammer Forging, Crankshaft of Ship Engine



A coupled analysis of both temperature and deformation was conducted for a hammer forging process in a ship engine using a counter-blow hammer forging machine for predicting the required number of blows.

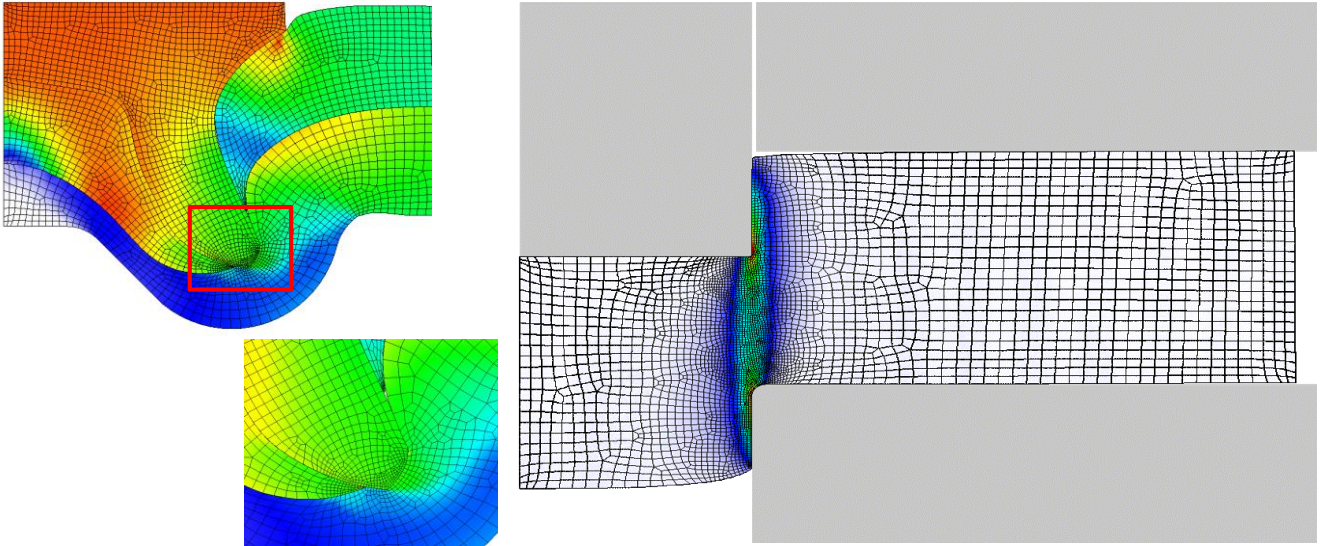
❖ 3D, Ring rolling, Polygonal Defect



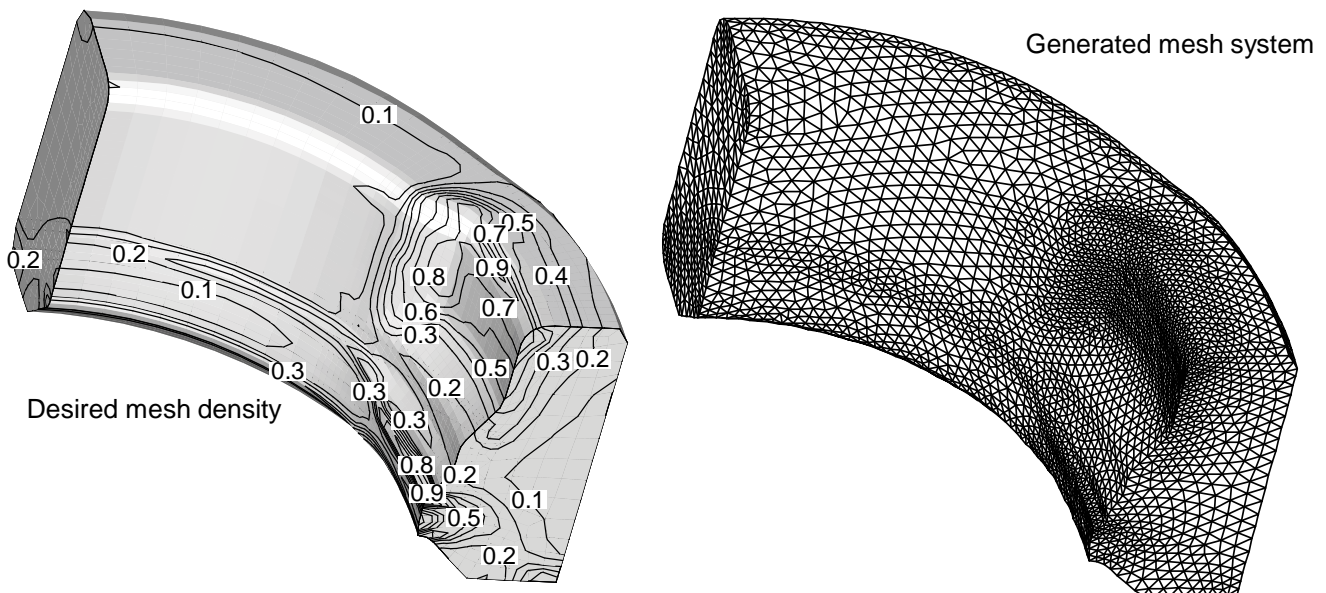
Polygonal shape defect formation is predicted, revealing that undesirable reduction with insufficient guiding load may cause various types of polygonal shape defects.

❖ Intelligent Remeshing

✓ 2D, Quadrilateral

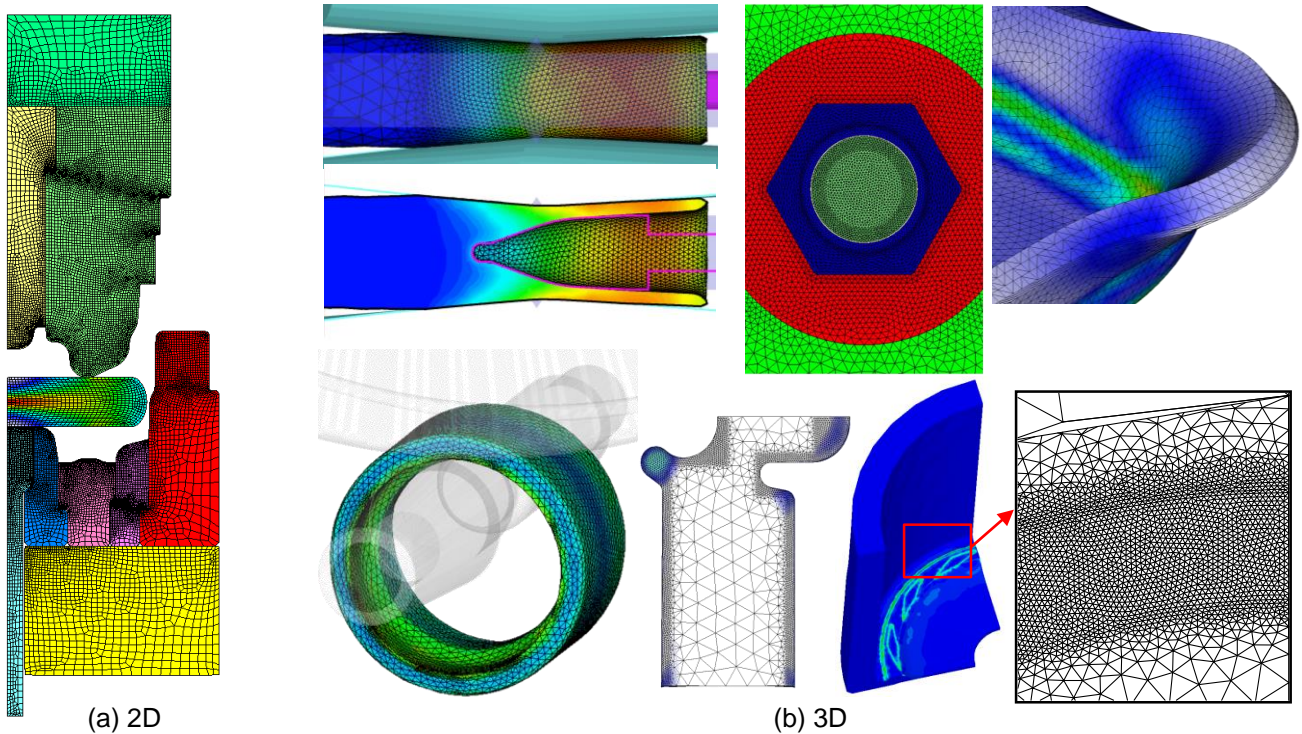


✓ 3D, Tetrahedral



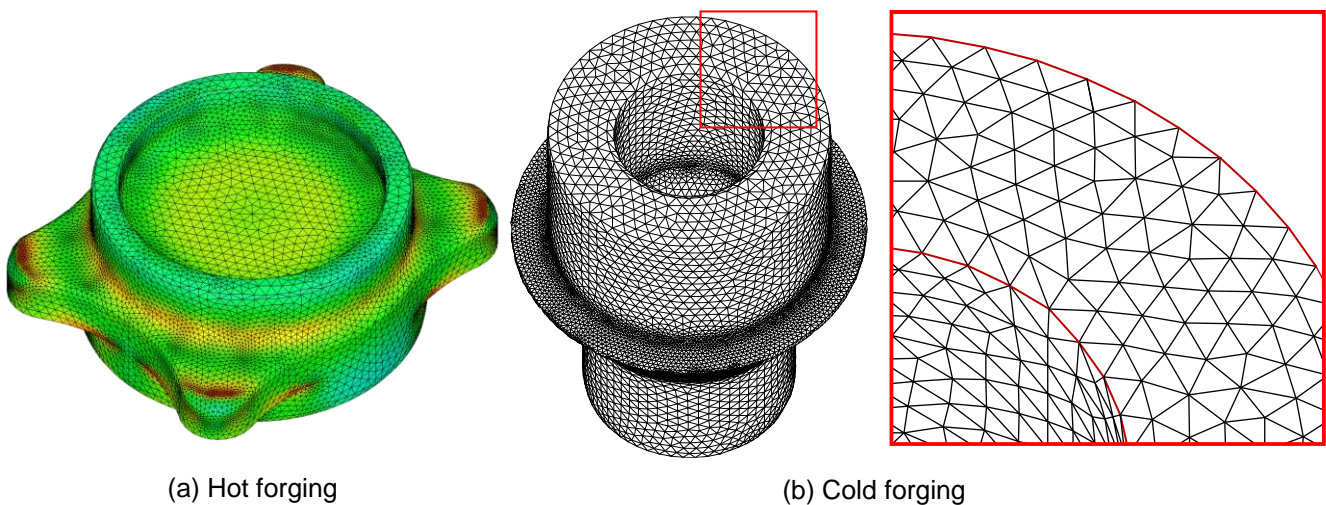
Two figures illustrate several typical quadrilateral and tetrahedral mesh systems, respectively. It should be emphasized that the deviation between the desired and generated mesh densities and the number of transition elements or regions is minimized during mesh generation or remeshing. Additionally, mesh quality (i.e., mesh regularity and normality near the workpiece-die interface) is optimized to reduce numerical inaccuracies. As lower figure illustrates, the mesh density of the generated tetrahedrons is in close agreement with the desired mesh density calculated using state variables just before remeshing, which is one of the biggest advantages of the automatic remeshing capability of AFDEX. These features help AFDEX to ensure solution accuracy and provide sophisticated simulations of precision BMF processes.

❖ Examples of Specially Constructed Mesh Systems



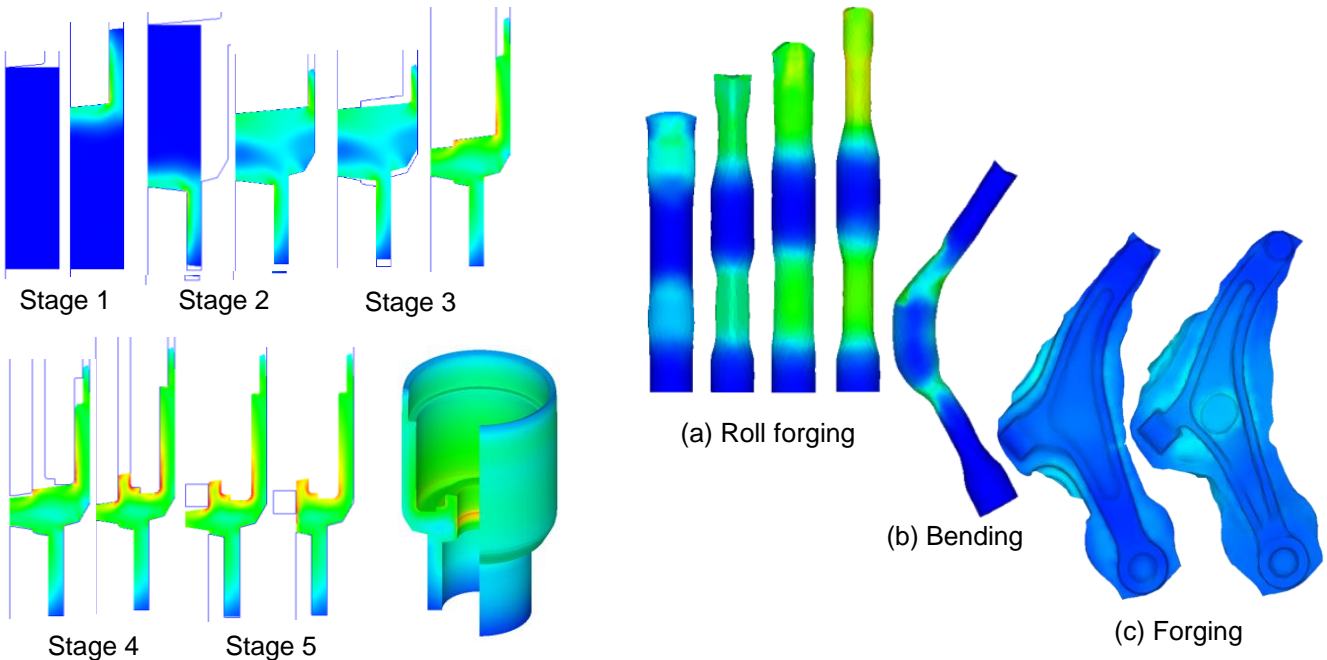
The mesh density for special problems can be manually set by users and a local remeshing capability is available that requires user intervention during remeshing. The figures show some specially constructed mesh systems during automatic and manual simulations.

❖ Sensitivity of Predictions near the Characteristic Boundaries or Edges



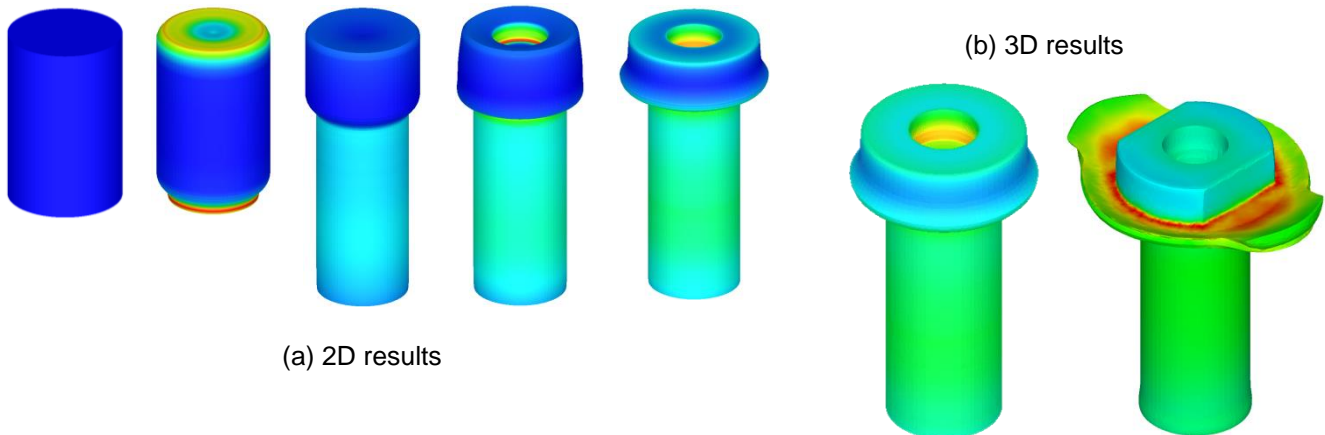
The figures show the edges generated in hot and cold forging, respectively. It should be emphasized that a detailed description of the workpiece geometry is a very important part of MFS if one is to obtain the sort of accurate results shown in the figures. The mesh system shown in Figure (b) describes the chamfered corner clearly and accurately with the limited number of tetrahedral elements. Description of such corner with greater number of elements should be avoided because frequent remeshing due to small volume of an element leads to greater numerical smoothing.

❖ 2D/3D, Fully Automatic Simulation



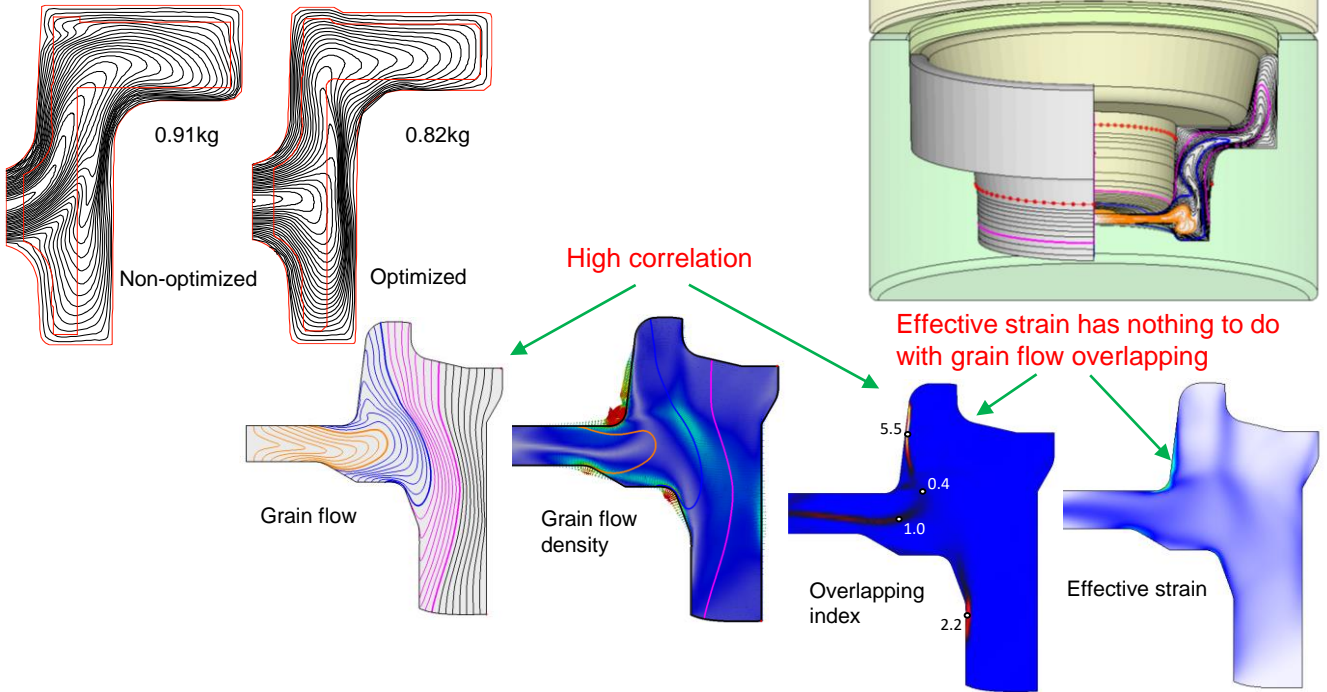
An intelligent forging simulator should have the capability of automatically simulating a sequence of multi-stage forging processes to minimize the total simulation time, including both computational time and user processing time between stages. Figures show predictions for an axisymmetric automatic five-stage cold forging process and a three-dimensional seven-stage compound hot metal forming process obtained using the automatic execution function of AFDEX 2D (left) and AFDEX 3D (right), respectively.

❖ 2D and 3D Combined Simulation

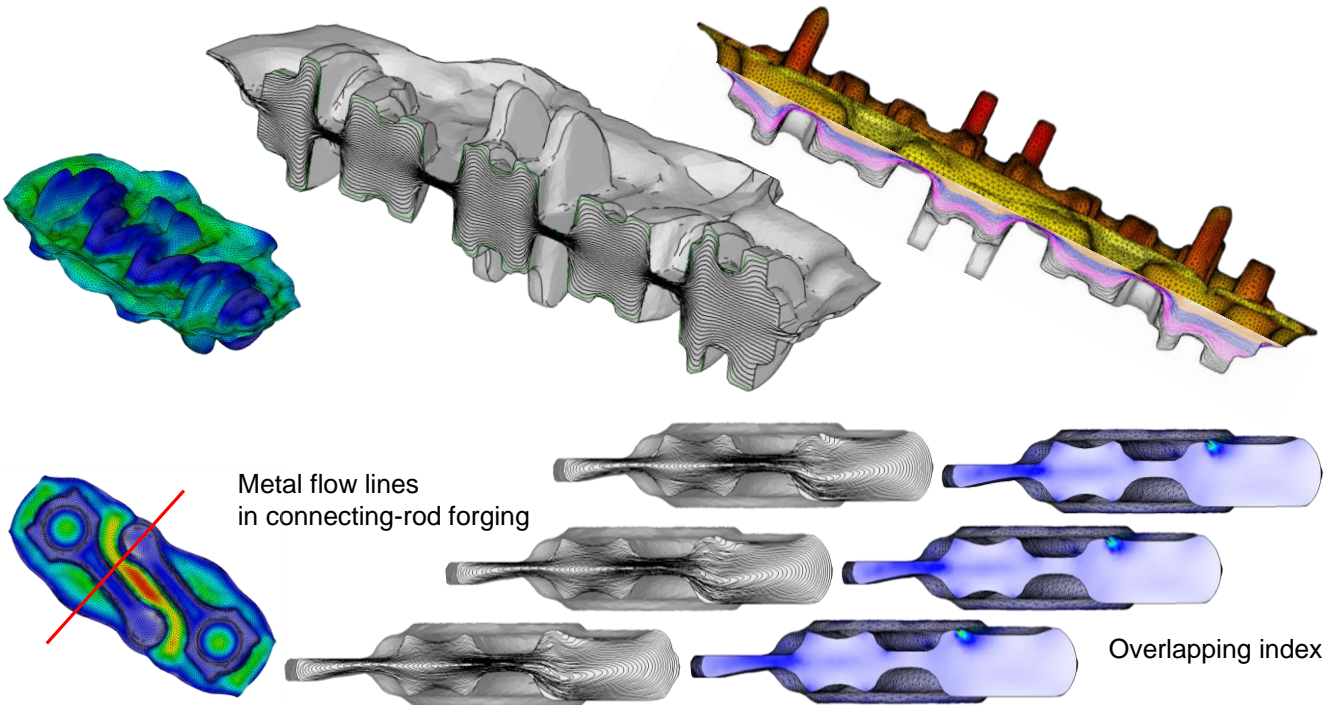


AFDEX 3D can read AFDEX 2D results files either directly or by means of a simple connecting program, and thus 2D and 3D combined simulations can easily be carried out. Of course, the 2D results can be viewed by the 3D post-processor with more powerful graphics functions. Figure shows the predictions of a five-stage precision cold forging process involving one piercing stage and a final three-dimensional stage, obtained by using the 2D and 3D combined simulation capability with minimum user intervention (i.e., with only an initial run and one connection run). It should be noted that this capability is especially efficient for fastener forming process simulation. The 2D and 3D combined simulation is strongly recommended for enhancing computational time, solution reliability, and engineering productivity when relatively few stages are three-dimensional.

❖ 2D Metal Flow Lines and Its Quantification



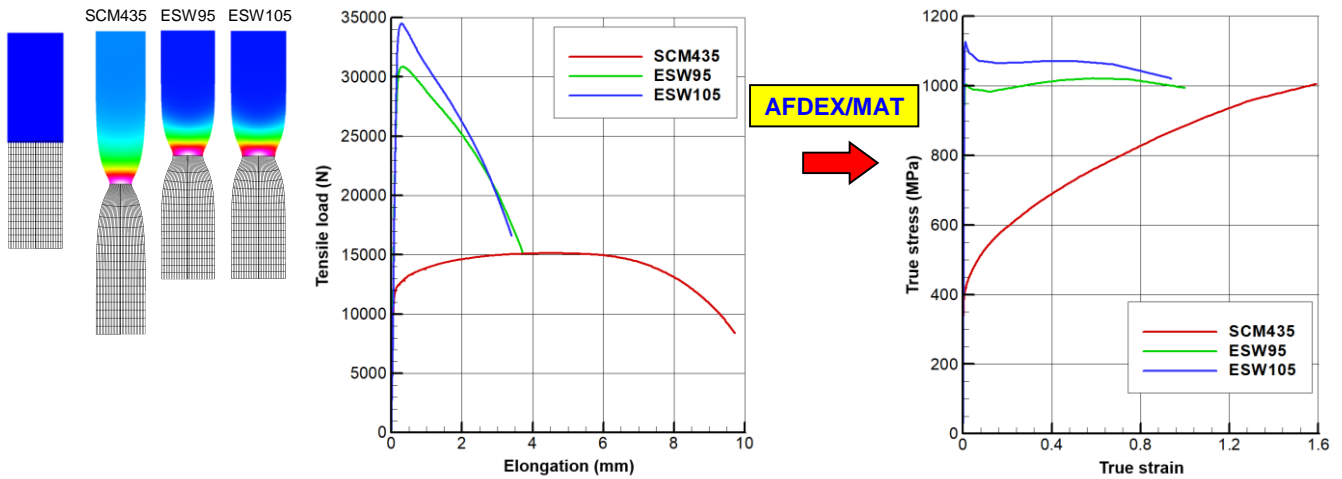
❖ 3D Metal Flow Lines and Its Quantification



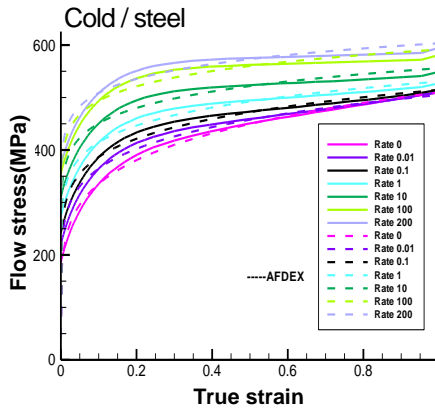
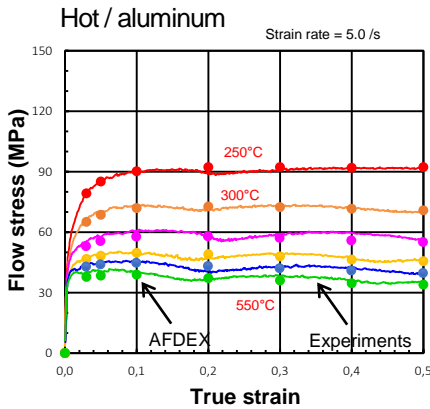
Metal flow line in metal formed products has a great influence on the strength of material and thus it is the most important factor in process design. Even an externally sound looking products often have decisive internal defects due to the bad metal flow lines. Therefore, one usually imposes some constraints on the internal metal flow line for most power transmission parts including gears, bearings and the like. Consequently, the precise prediction of metal flow line and its convenient visualization become highly important. AFDEX is powerful in this field as shown in the figures, which shows 2D and 3D metal flow line formed during metal forming processes.

❖ Material Identification

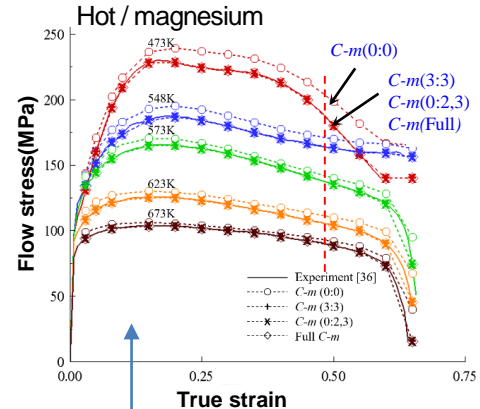
✓ Tensile test at the room temperature – Improved Hollomon’s model



✓ Power Law Model (C-m)



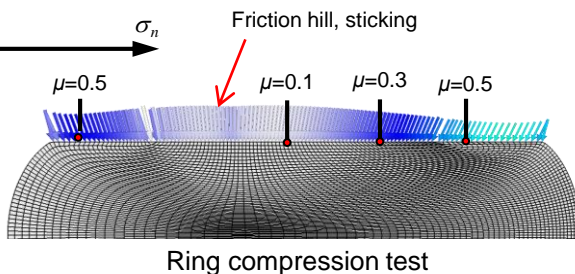
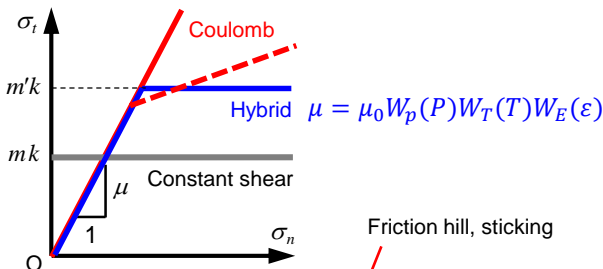
✓ Generalized Power Law Model



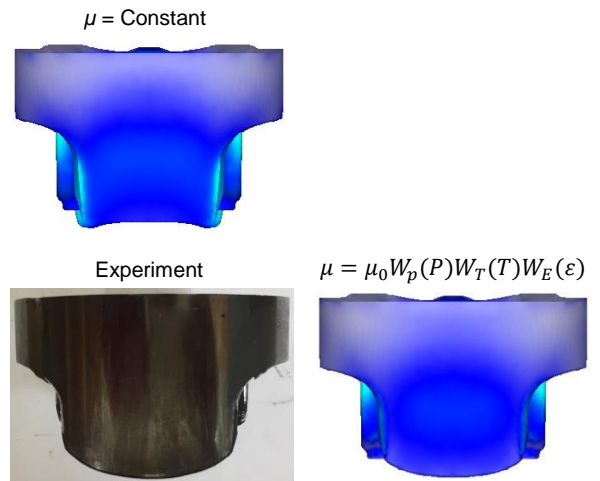
Any flow curve can be expressed accurately.

❖ Sophisticated Frictional Laws

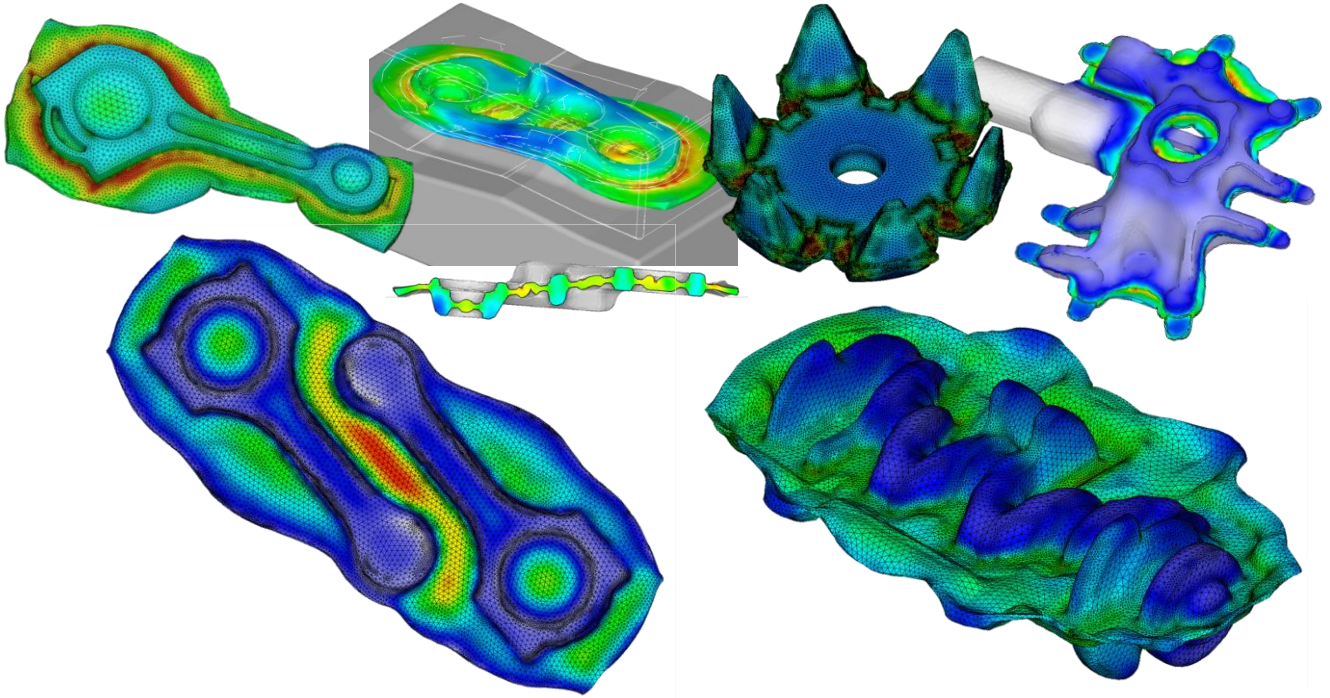
✓ Law of frictions



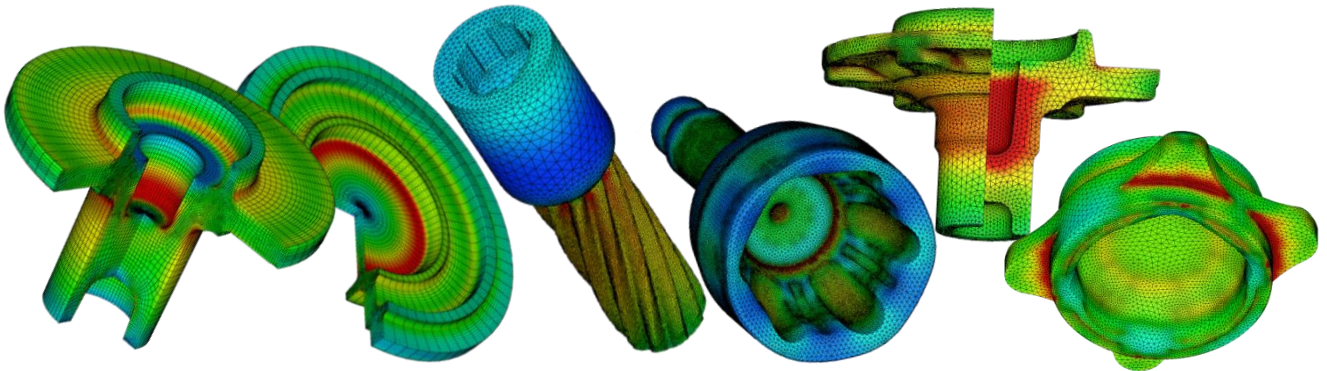
✓ Identification of Frictional Condition



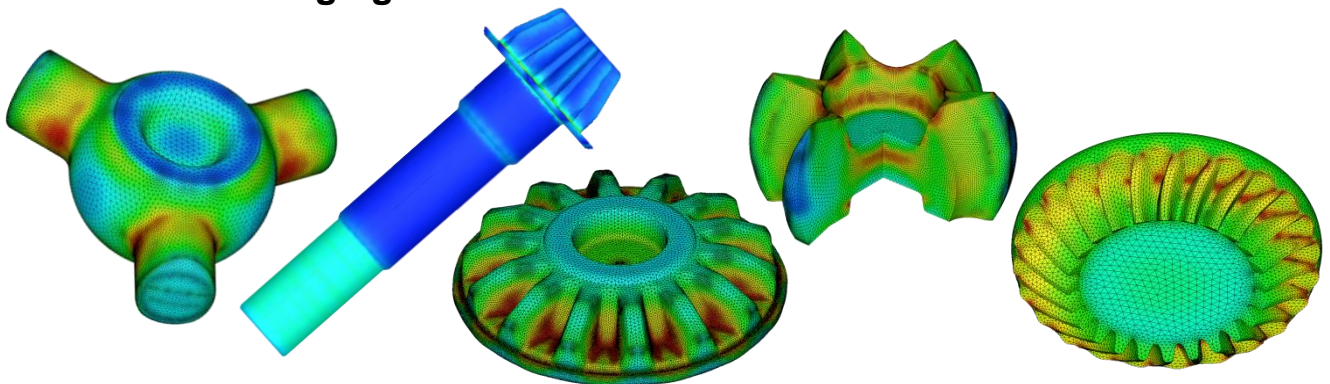
❖ Closed Die Forging with Flash



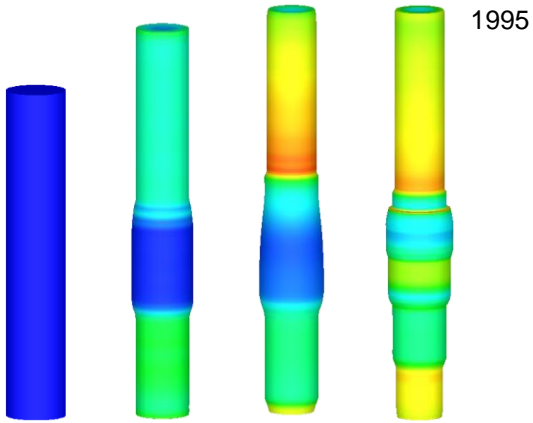
❖ Closed Die Forging without Flash



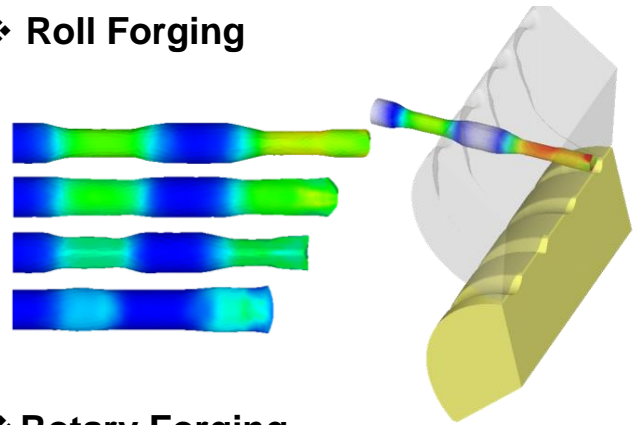
❖ Enclosed Die Forging



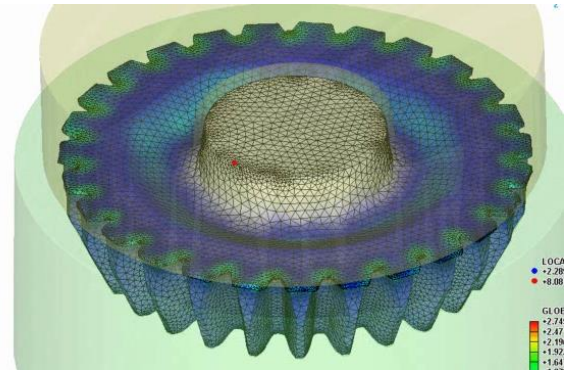
❖ Automatic Multi-stage Forging



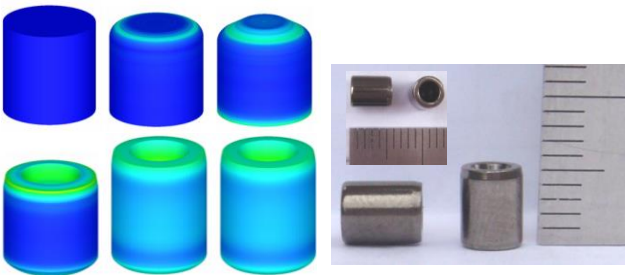
❖ Roll Forging



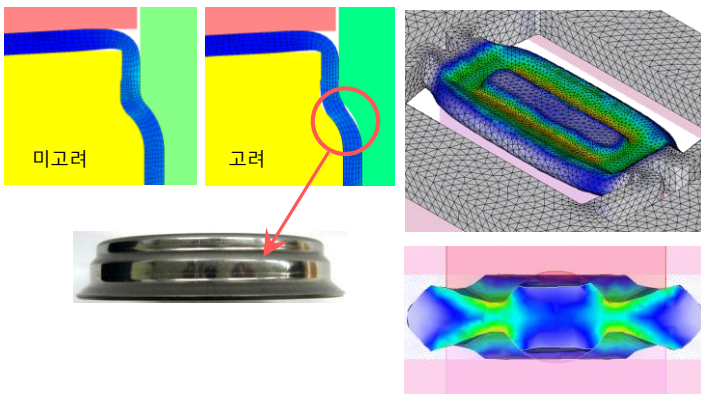
❖ Rotary Forging



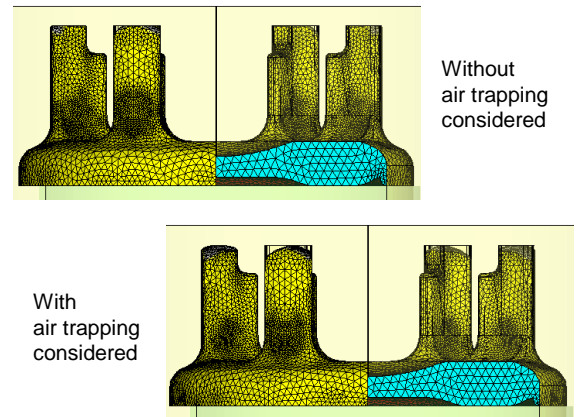
❖ Micro-forming



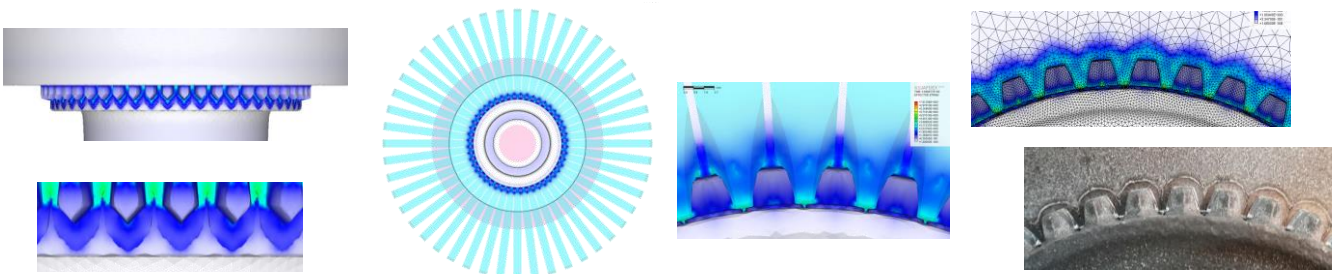
❖ Plate Forging with Air-trapping



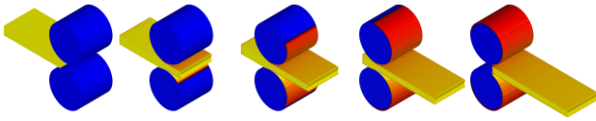
❖ Forging Process with Air-trapping



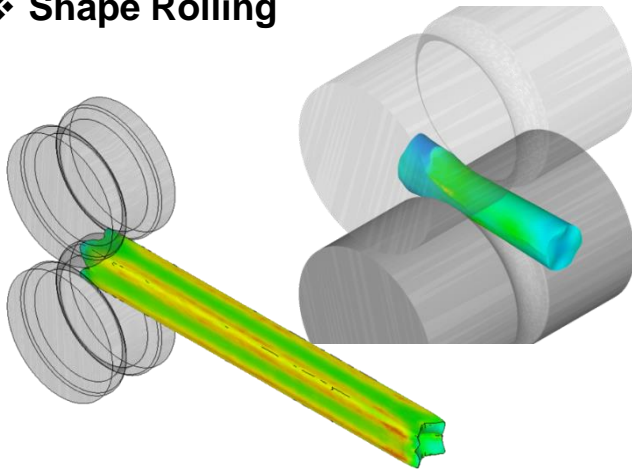
❖ Precision Simulation of Speed Gear



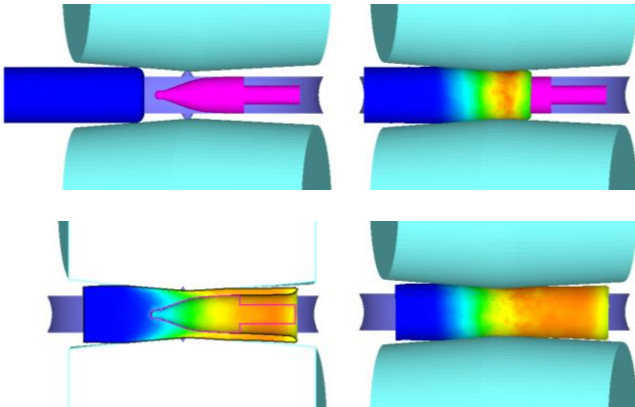
❖ Strip or Plate Rolling



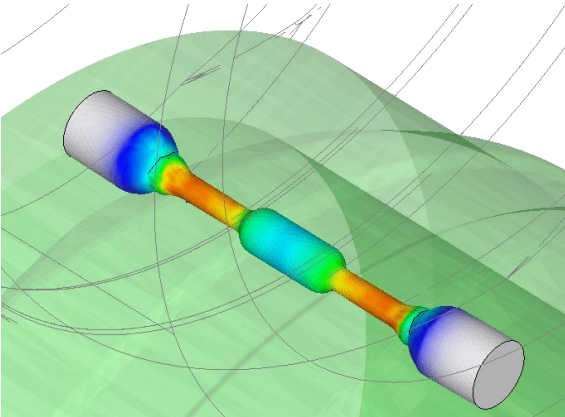
❖ Shape Rolling



❖ Roll Piercing



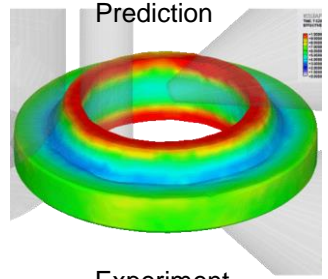
❖ Cross Wedge Rolling



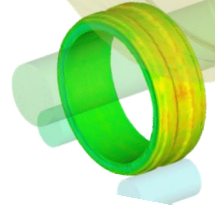
❖ Ring Rolling



Profiled ring



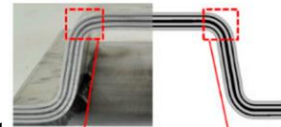
Prediction



Experiment

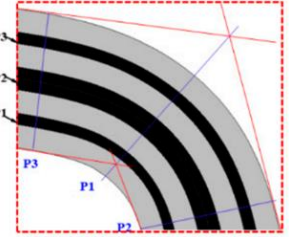
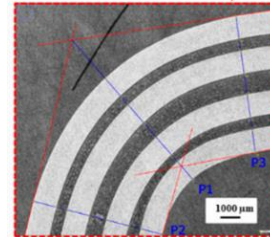


❖ CFRP

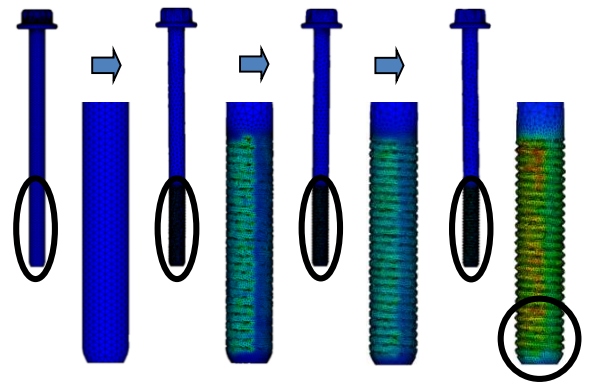


Experiment

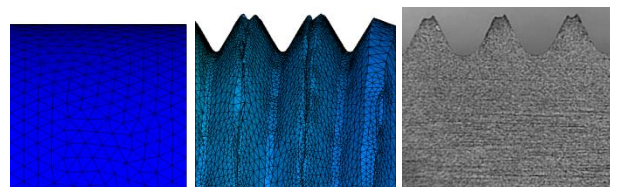
Prediction



❖ Thread Rolling

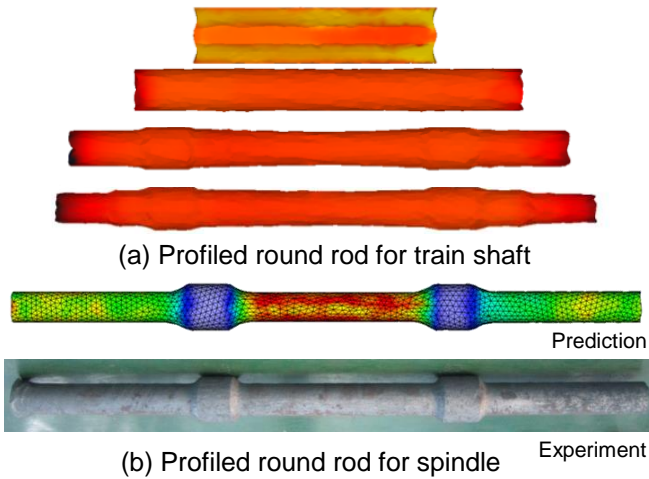


Entire model

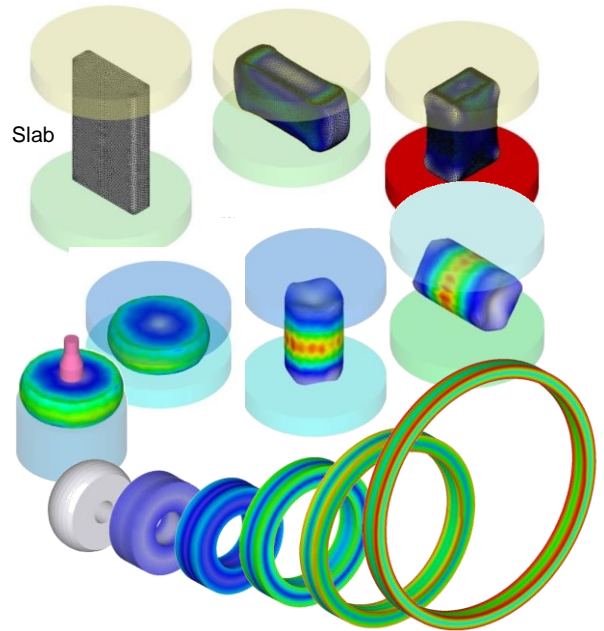


Local model

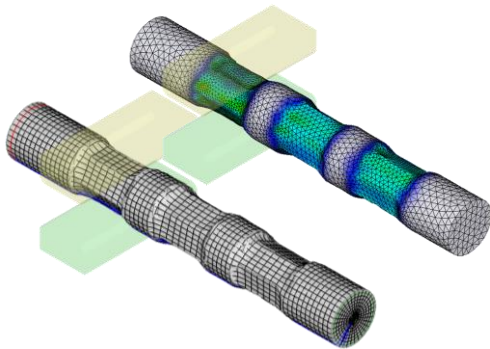
❖ Radial Forging of Stepped Bar



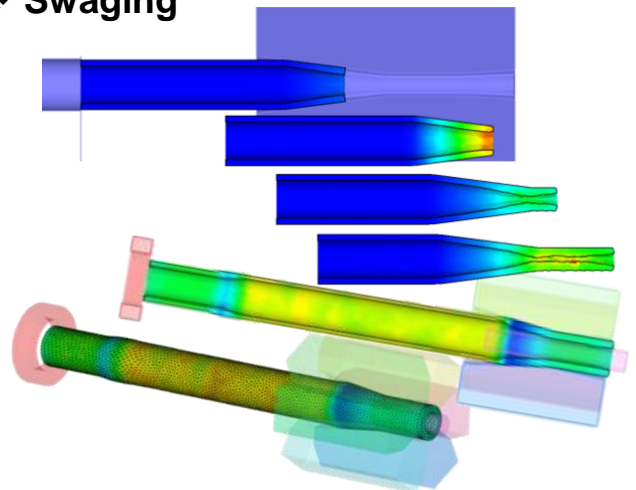
❖ Open-die Forging



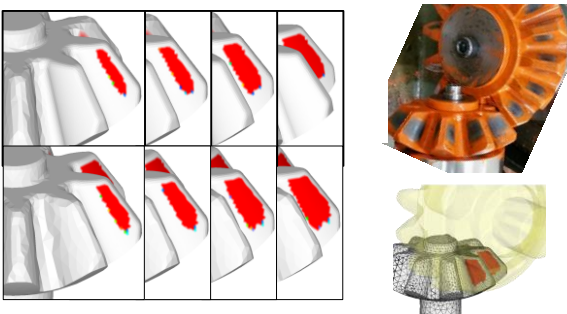
❖ Open-die Hammer Forging



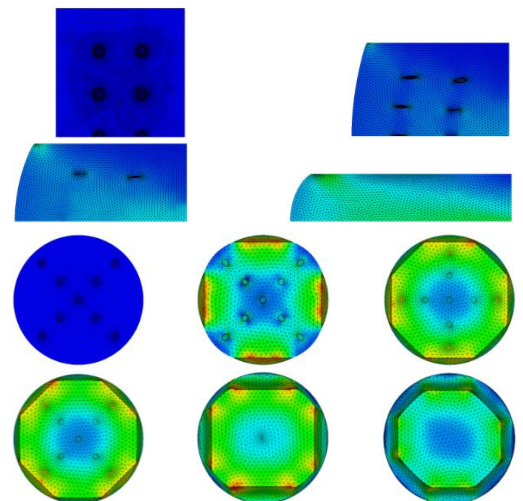
❖ Swaging



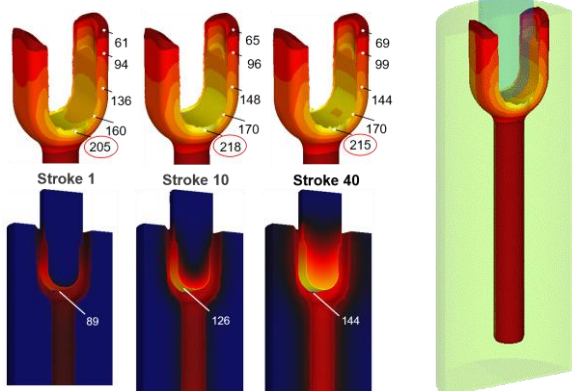
❖ Gear Contact Analysis



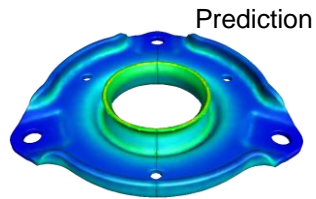
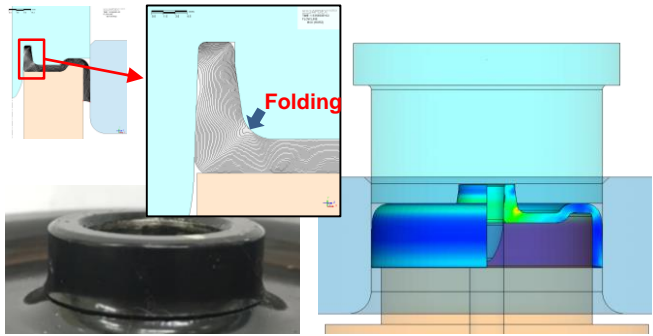
❖ Pore Closing during Upsetting



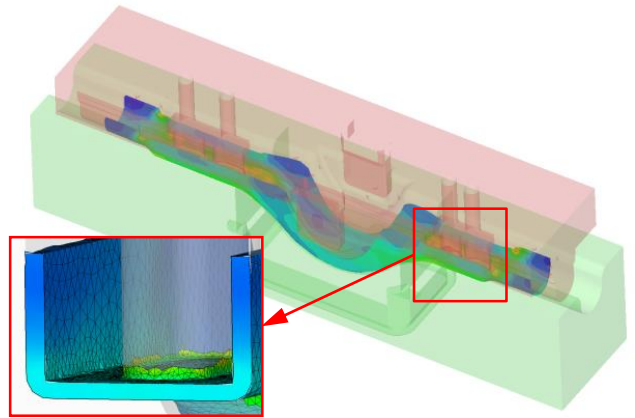
❖ Recursive Analysis



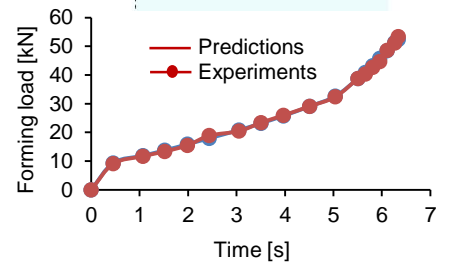
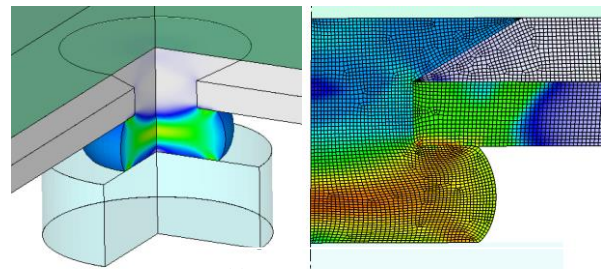
❖ Cold Plate Forging



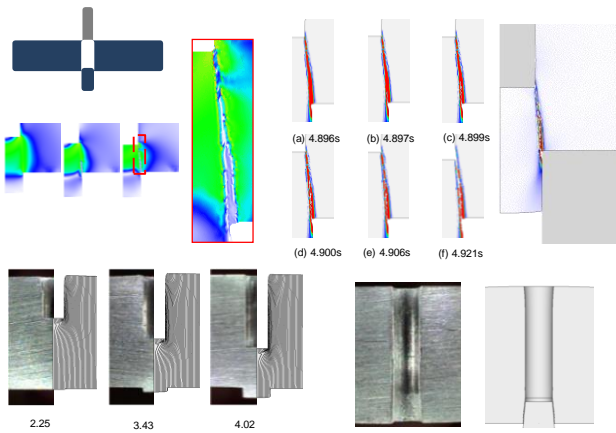
❖ Hot Plate Forging



❖ Riveting Process

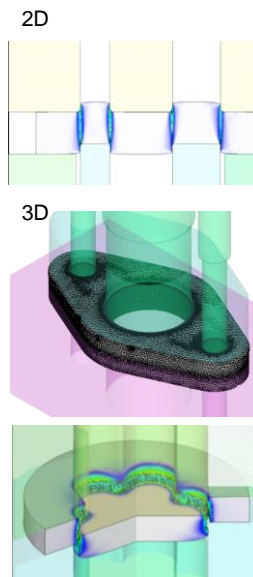


❖ Deep Piercing

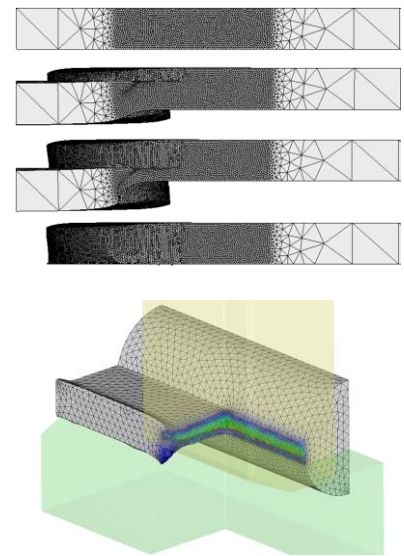


❖ Piercing or Trimming

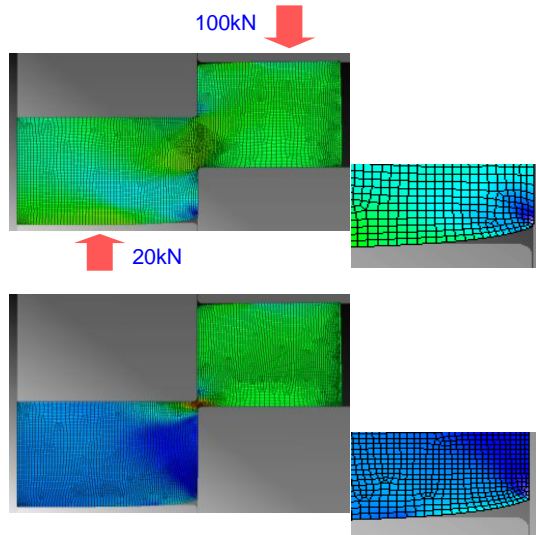
(a) Piercing



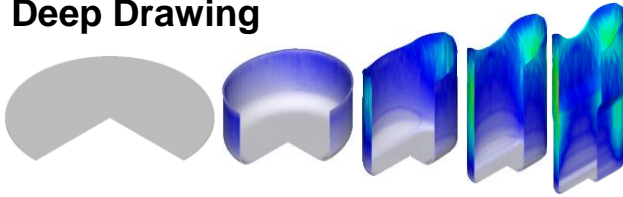
(b) Trimming



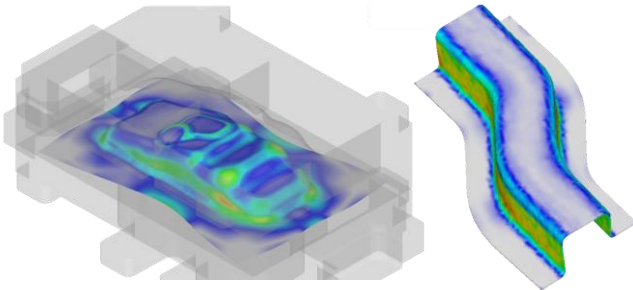
❖ Fineblanking



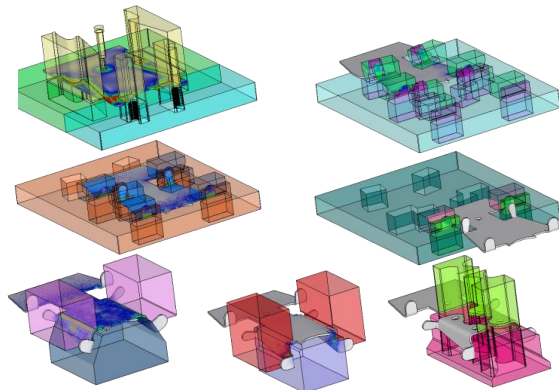
❖ Deep Drawing



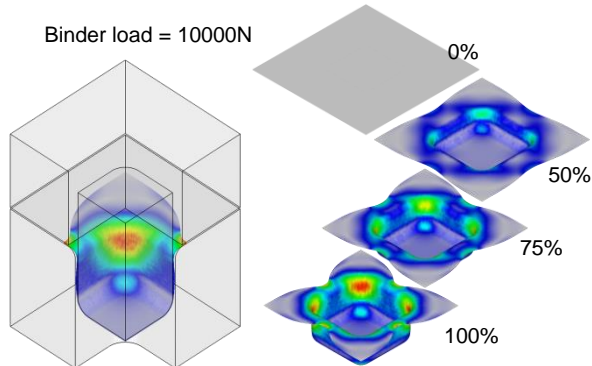
❖ Bulk Metal Forming Simulation Method of Sheet/Plate



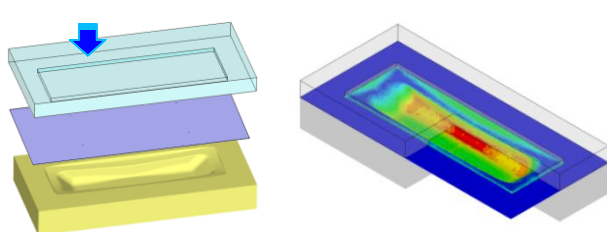
❖ Progressive Forming



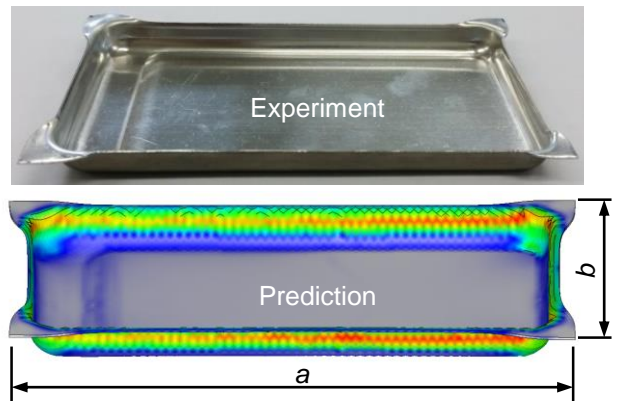
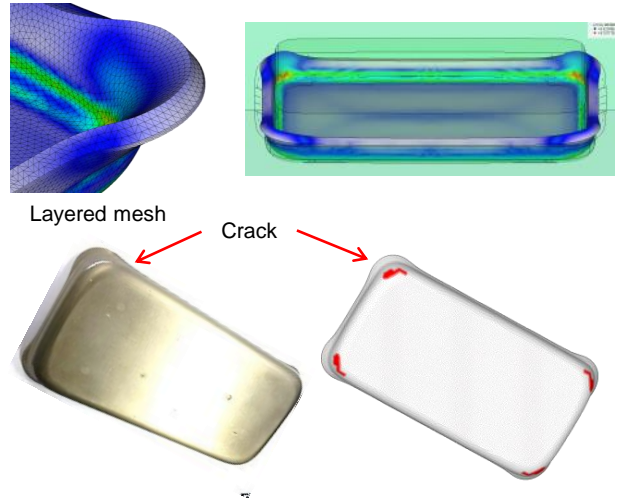
❖ Square-cup Deep Drawing



❖ Superplastic Forming

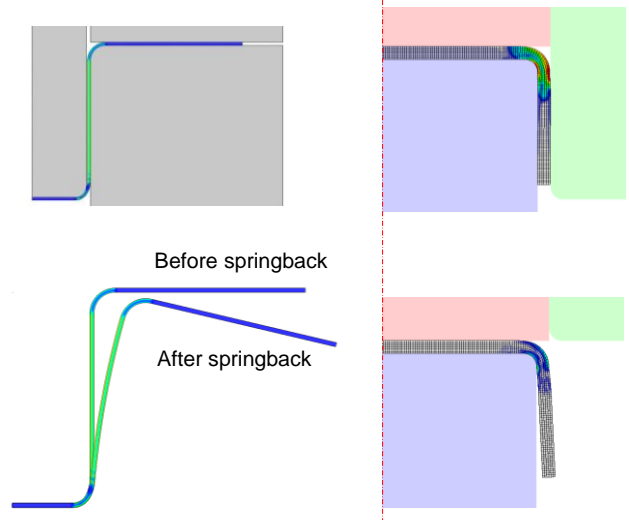


❖ Clad-metal Plate Forming

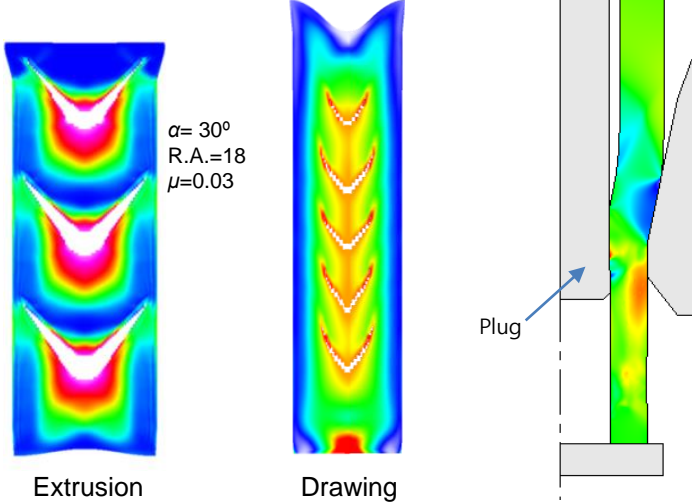


	<i>a</i> (mm)	<i>b</i> (mm)
Experiment	126.9	67.9
Prediction	126.7	68.3

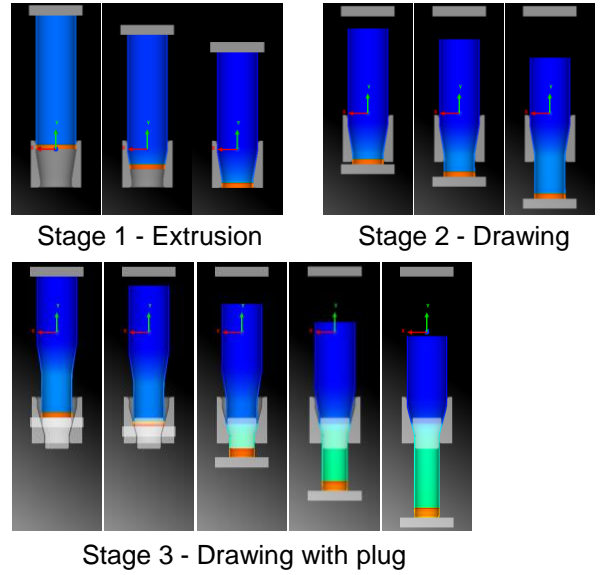
❖ Springback Analysis



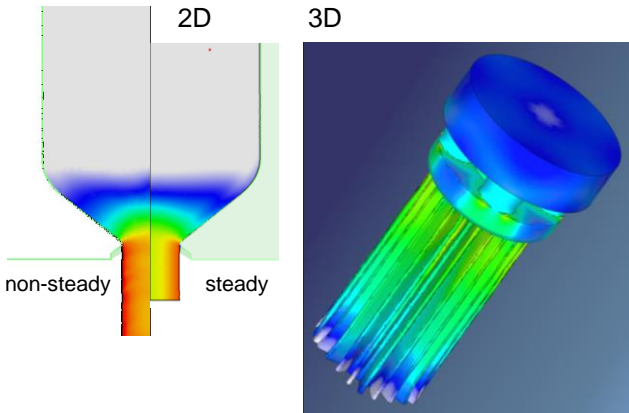
❖ Extrusion and Drawing with Central Bursting Cracks



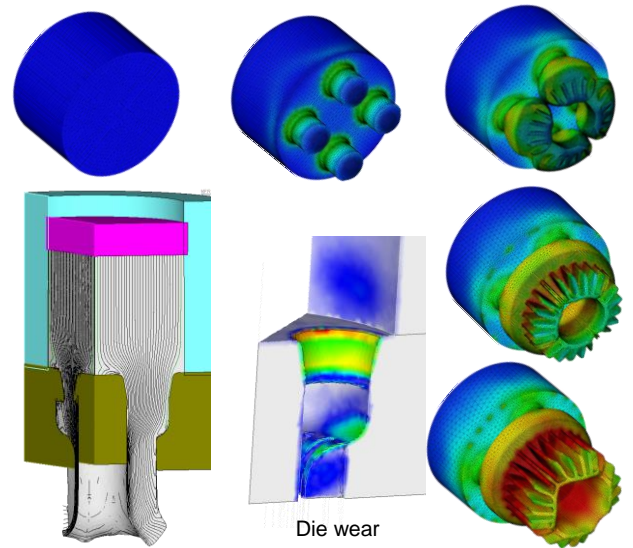
❖ Tube Drawing with Back Pressing



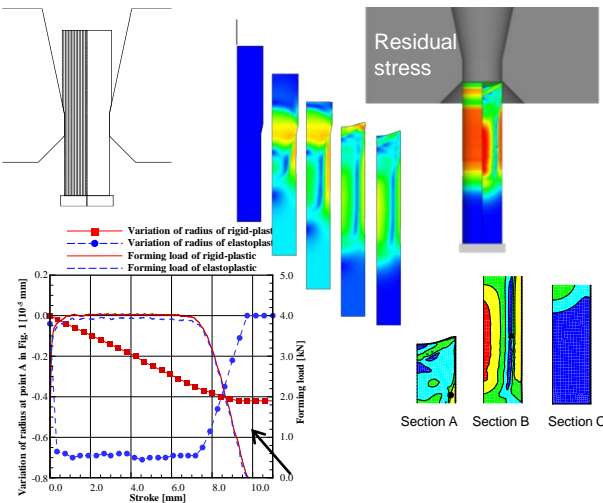
❖ Steady-state Extrusion



❖ Porthole Extrusion

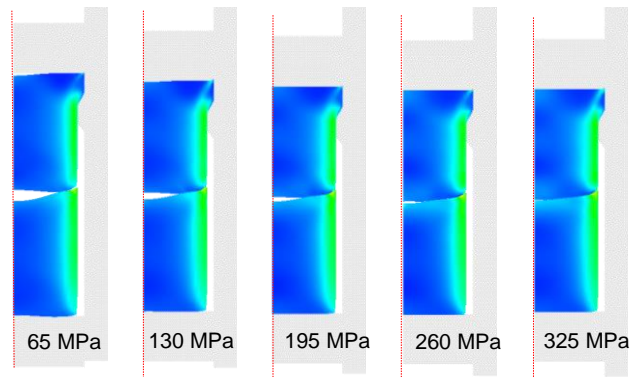


❖ Residual Stress Analysis

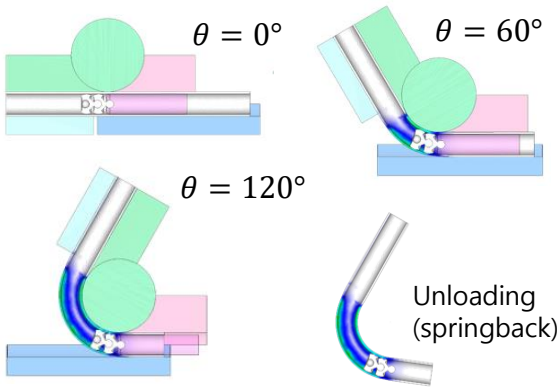


Elastoplastic FEA function of AFDEX was evaluated using a drawing process, and it turned out that the predicted results agreed well with theory.

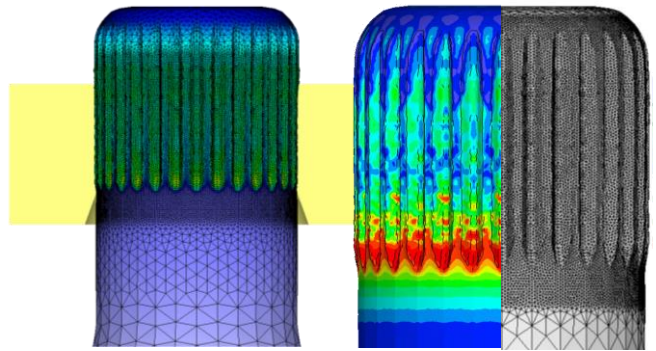
❖ Multi-object Extrusion with Back Pressure Applied



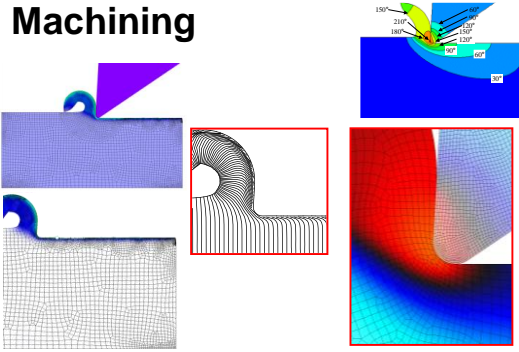
❖ Pipe Bending



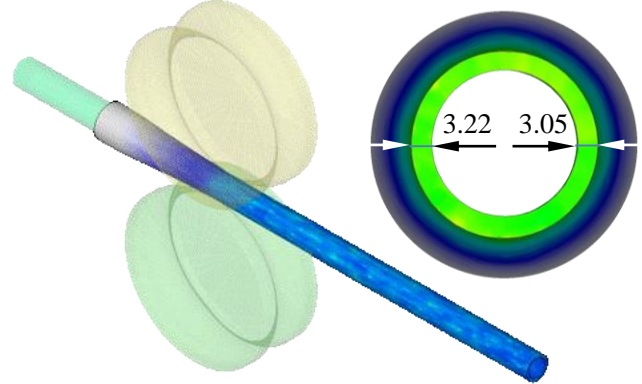
❖ Forming using Oscillatory Die



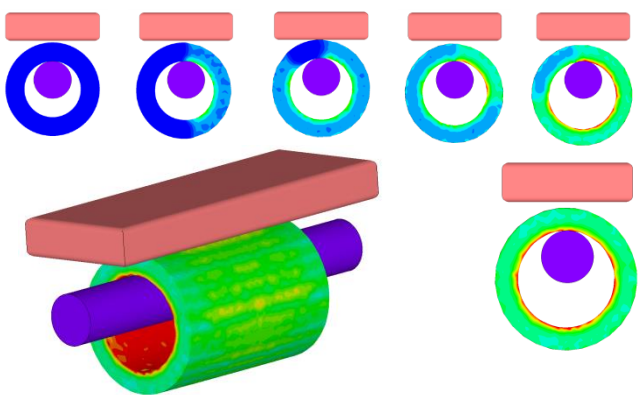
❖ Machining



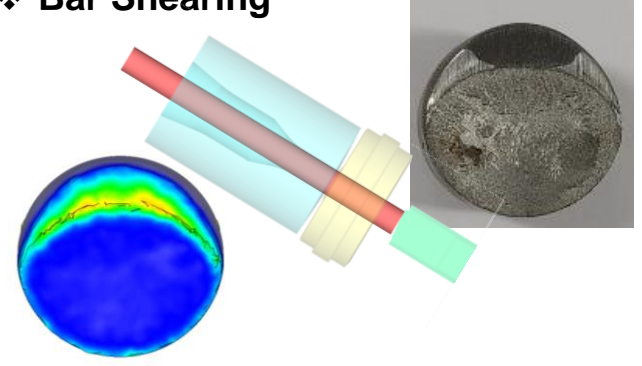
❖ Pilgering



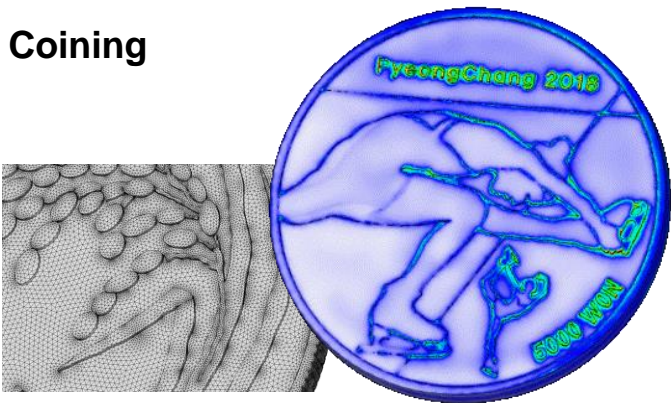
❖ Hollow Cylinder Expanding



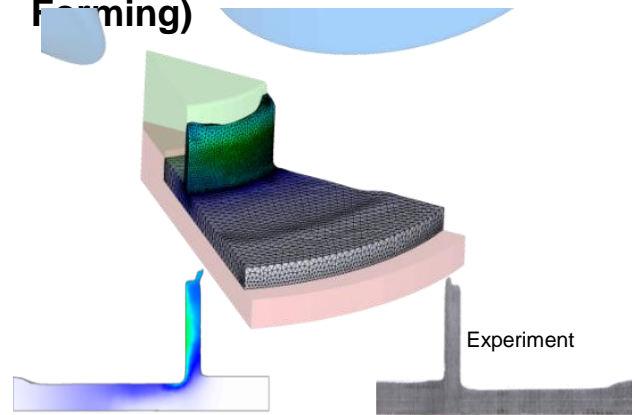
❖ Bar Shearing



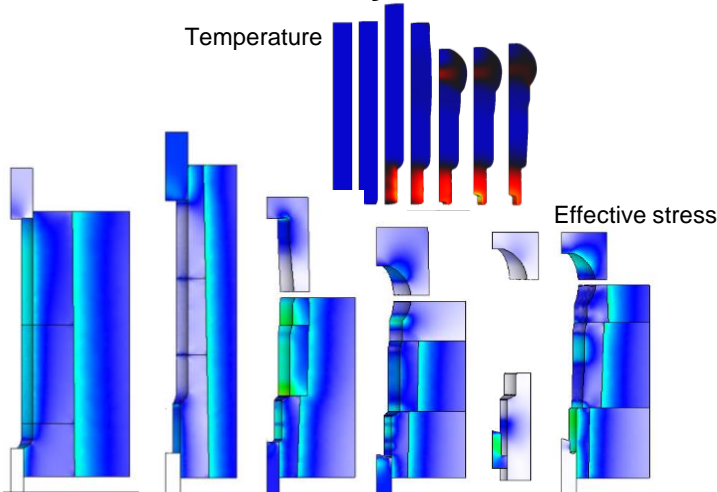
❖ Coining



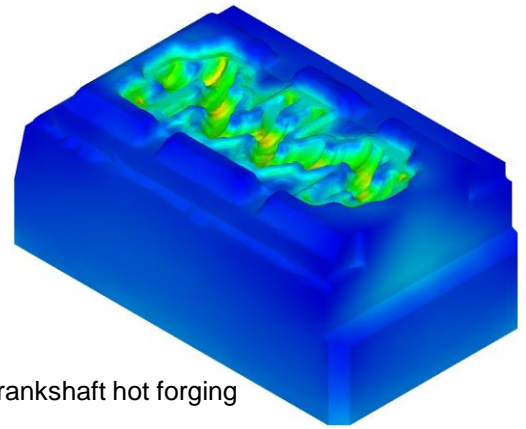
❖ Chipless Forming (Flow Forming)



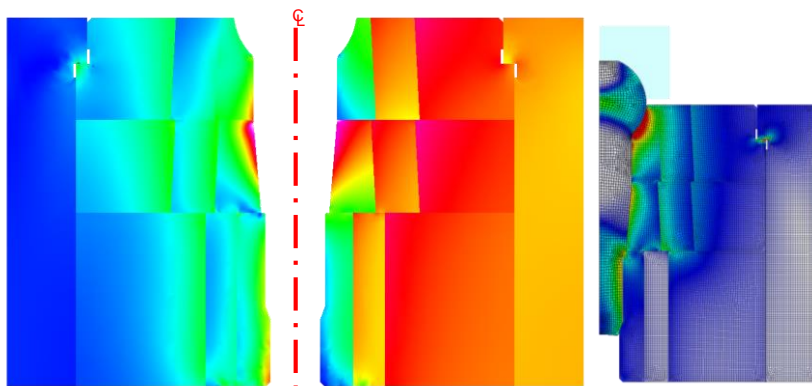
❖ Die Structural Analysis



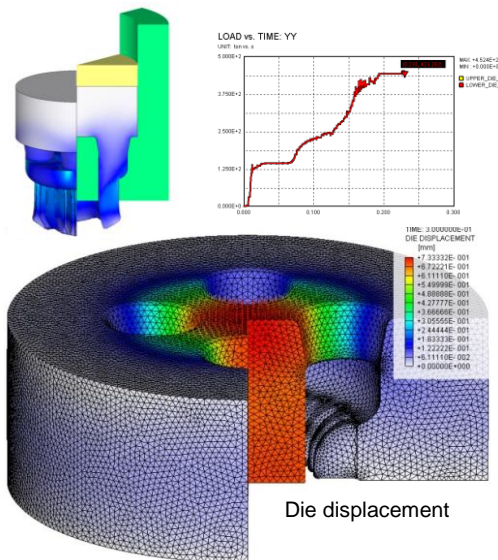
(a) Cold forging, SUS 304, ball-stud



(b) Crankshaft hot forging



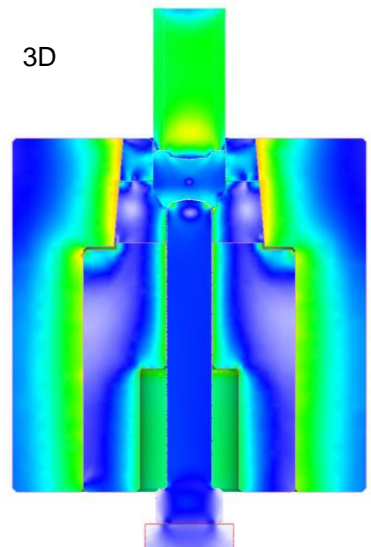
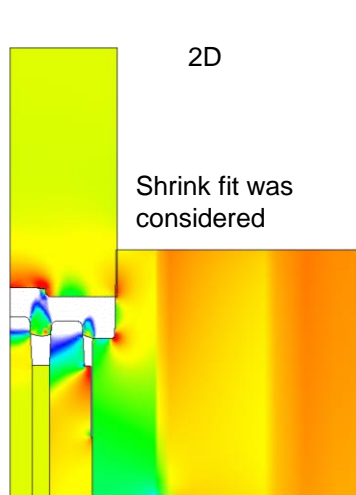
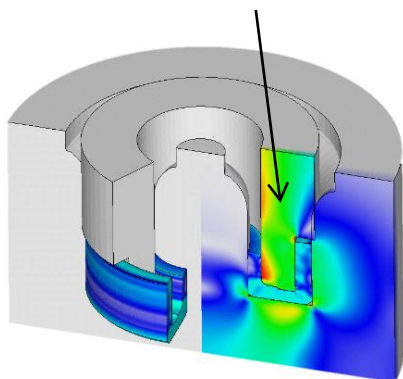
(c) Cold forging, die, ball-stud



(d) Coupled analyses of deformations of die and material in a port-hole extrusion

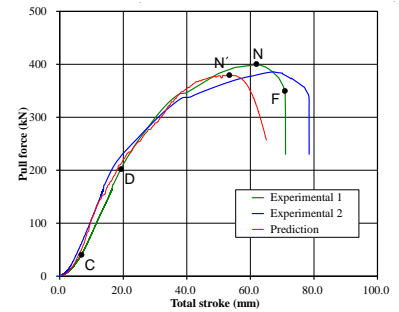
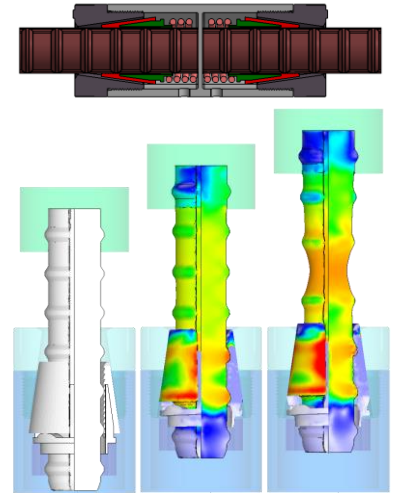
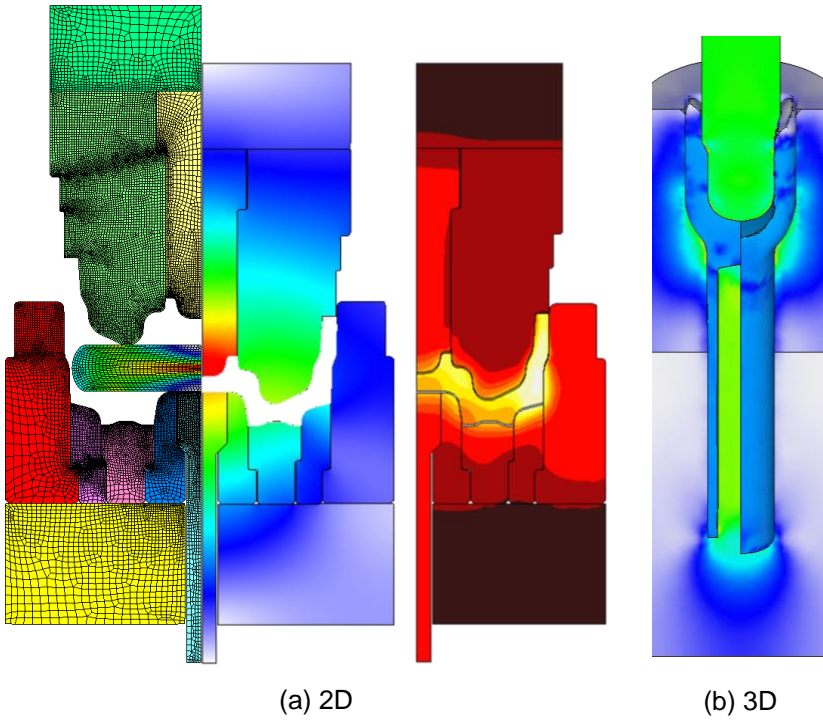
❖ Precision Forging Simulation (Complete Simulation) considering Effect of Die Elastic Deformation and Shrink Fit

It is essential for precision forging simulation to consider a die deformation, especially around here.

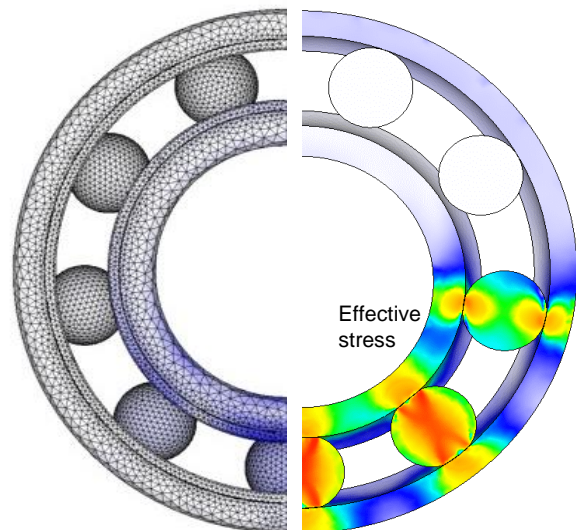
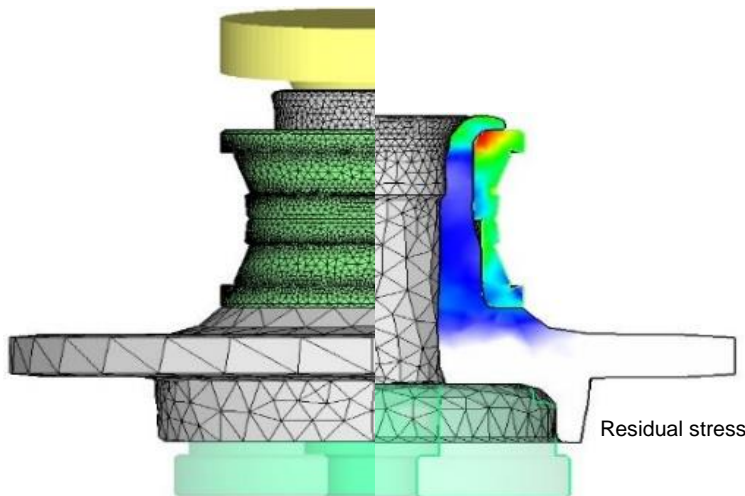
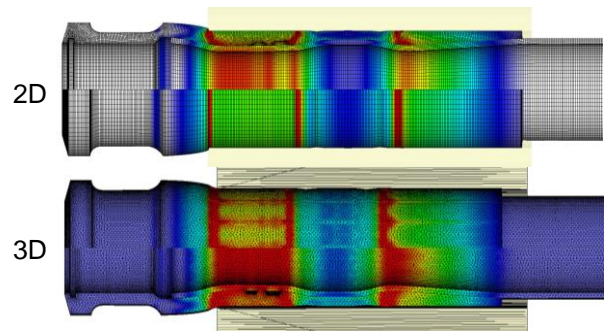
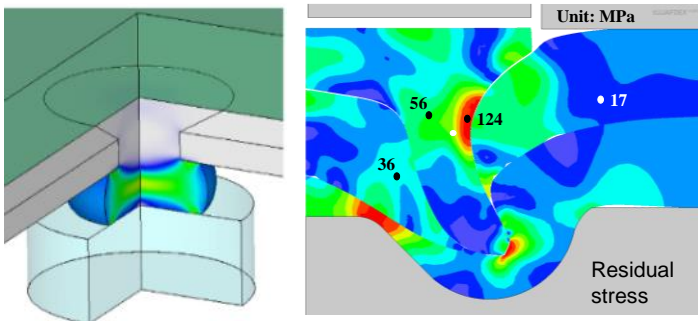


❖ Multi-piece Die Forging Process Simulation

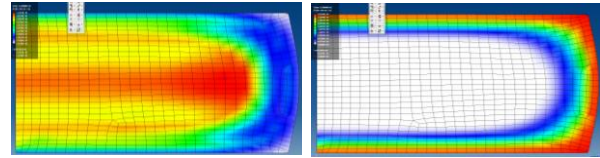
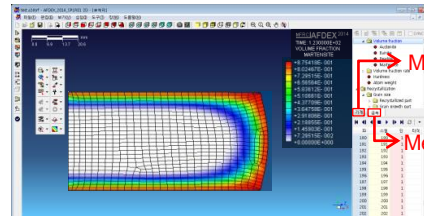
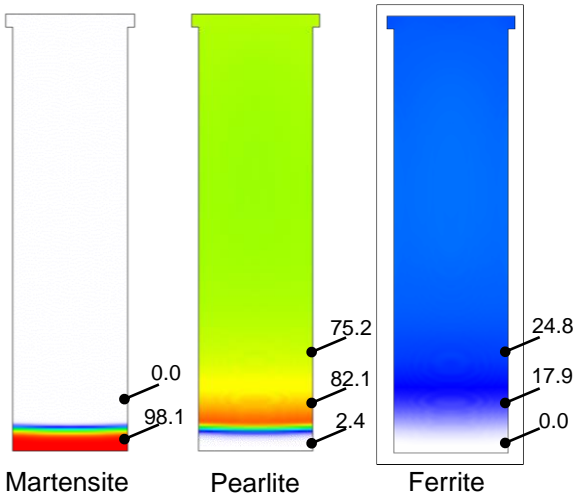
❖ Assembly Strength Testing



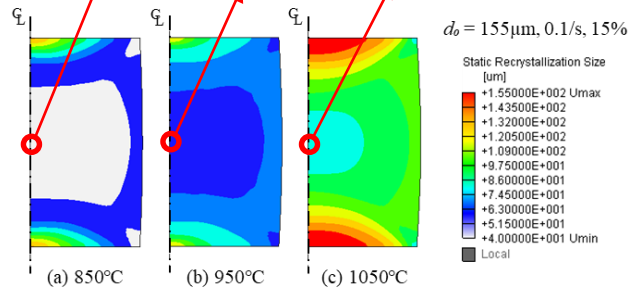
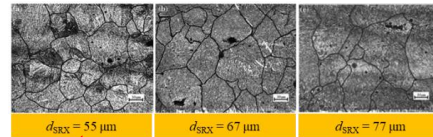
❖ Multi-body Forging Process Simulation



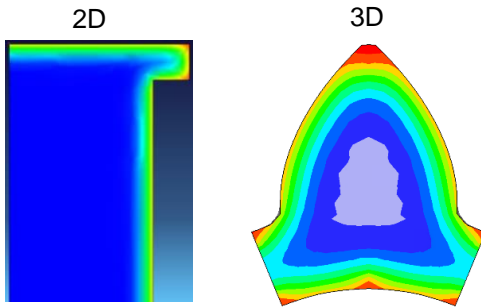
❖ Heat Treatment Analysis with Phase Transformation



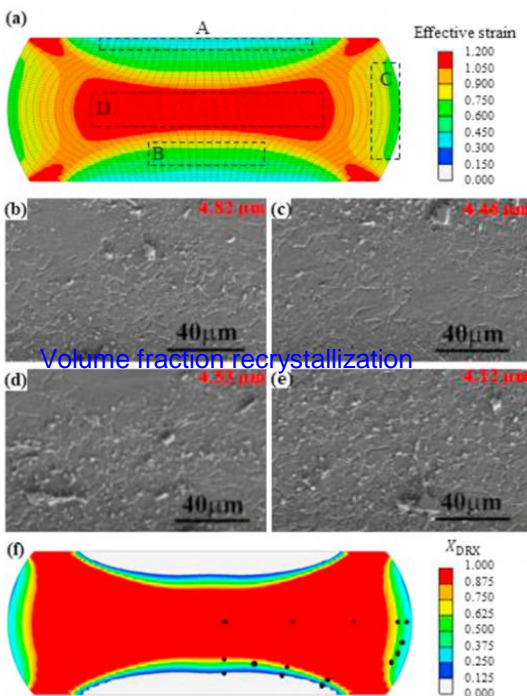
❖ Prediction of SRX Microstructure



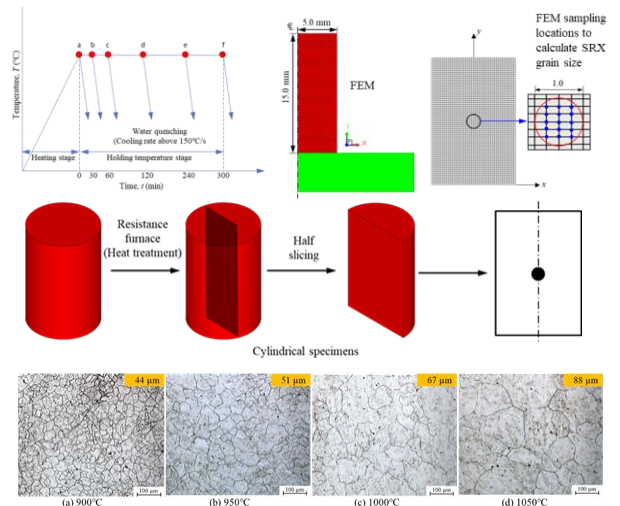
❖ Carburation/ Hardness Prediction



❖ Prediction of DRX Microstructure



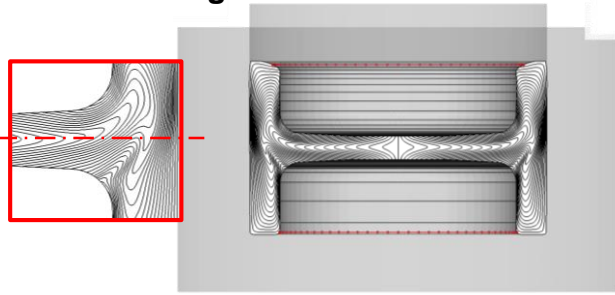
❖ Prediction of Grain Growth



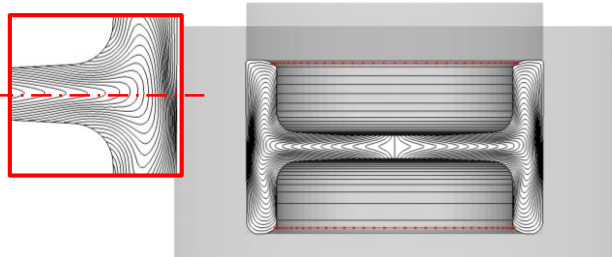
Experimental microstructure depending on temperature

❖ Optimal Process Design for Metal Flow Lines (MFL)

✓ Initial design

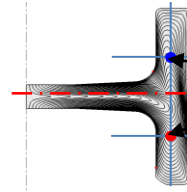


✓ Optimized design

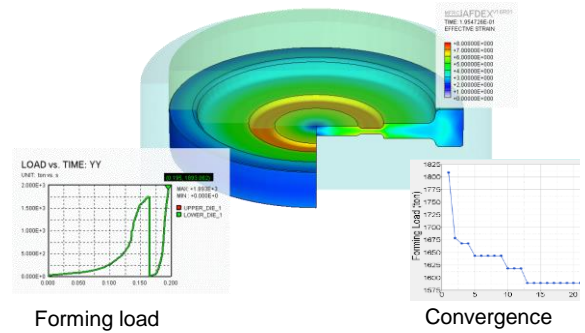


✓ Objective function

Difference between MFL function values at blue and red points

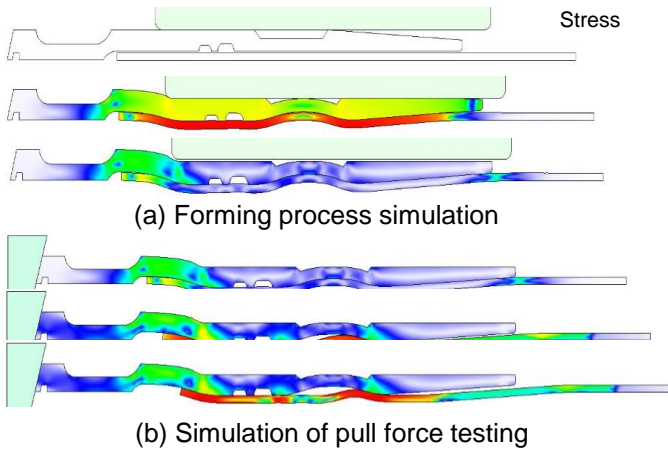


❖ Optimal Process Design, Forming Load



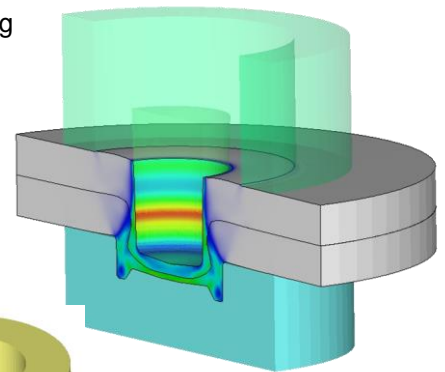
❖ Optimal Process Design, Capacity

✓ Optimized process design

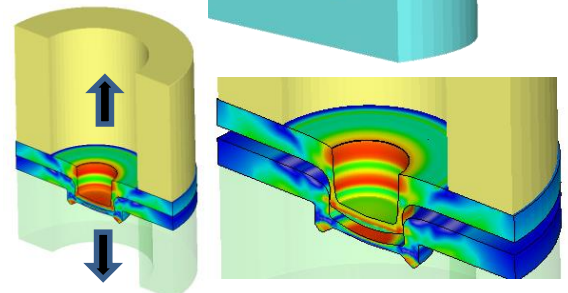


❖ Optimal Process Design of Clinching, Joint Strength

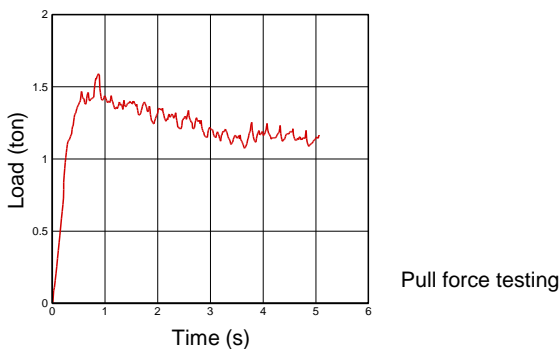
(a) Forming



(b) Joint strength testing



✓ Pulling Force of Tube from Assembly





A1208, WingsTower, 12, Dongbu-ro 169, Jinju, Korea, 52818
TEL. +82-55-755-7529 mfrc@afdex.com www.afdex.com



Dennewartstr. 25-27 | 52068 Aachen | Germany
TEL. +49-241-963-1680 sales@morphotec.de www.morphotec.de